In presenting the dissertation as a partial fulfillment of the requirements for an advanced degree from the Georgia Institute of Technology, I agree that the Library of the Institute shall make it available for inspection and circulation in accordance with its regulations governing materials of this type. I agree that permission to copy from, or to publish from, this dissertation may be granted by the professor under whose direction it was written, or, in his absence, by the Dean of the Graduate Division when such copying or publication is solely for scholarly purposes and does not involve potential financial gain. It is understood that any copying from, or publication of, this dissertation which involves potential financial gain will not be allowed without written permission.

_____

7/25/68

# NUCLEAR DECAY SCHEME STUDIES USING RADIATIVE CAPTURE OF THERMAL NEUTRONS

A THESIS

Presented to

The Faculty of the Graduate Division

by

John Wiley Lewis III

In Partial Fulfillment

of the Requirements for the Degree

Doctor of Philosophy

in the School of Physics

Georgia Institute of Technology

August, 1971

# NUCLEAR DECAY SCHEME STUDIES USING RADIATIVE CAPTURE OF THERMAL NEUTRONS

Approved: _____

_____

Chairman

_____

_____

Date approved by Chairman: _____

# ACKNOWLEDGMENTS

The author would like to thank Dr. D. A. McClure, under whose supervision this work was done, for his encouragement and advice. The teaching and example of Dr. C. H. Braden led to the author's interest in experimental nuclear physics, and his continuing help and stimulation are greatly appreciated. Dr. E. T. Patronis and Professor N. S. Kendrick were always willing not only to help but also to explain. Dr. L. D. Wyly contributed to the present research in many ways, and the comments of Dr. G. G. Eichholz were most helpful.

The staff of the Georgia Tech Research Reactor was cooperative and patient. Mr. Jerome Callahan contributed greatly to the construction of the experimental apparatus.

The continuing support of the School of Physics is appreciated. A National Science Foundation Predoctoral Traineeship allowed the last year of thesis research to proceed more smoothly.

Thanks are due Miss Wynette Wright for her careful, prompt typing of the final draft of this thesis.

TABLE OF CONTENTS

TABLE OF CONTENTS (Continued)

# LIST OF TABLES

# LIST OF ILLUSTRATIONS

# SUMMARY

The radiative capture of thermal neutrons yields gamma rays whose energies, intensities, and coincidence relationships provide information about the structure of the product nucleus. A radiative capture facility was constructed at the Georgia Tech Research Reactor and used in the study of several nuclear decay schemes. This thesis reports data from thermal neutron capture in $^{77}$Se and presents a decay scheme for $^{78}$Se based on this data and on information from previous charged-particle and radioactive decay work.

The thermal capture facility consisted of a collimated, filtered external neutron beam with a flux of $4 \times 10^6$ n/cm$^2$-sec and a diameter of 1.25 cm. Ge(Li) detectors were used exclusively in both singles and coincidence gamma ray spectroscopy. In coincidence work data from two detectors were recorded in a multiparameter magnetic tape data acquisition system as a 4096 by 4096 channel array. A digital computer program sorted these data and produced spectra of those events in one detector which were in coincidence with gamma rays in a narrow energy region in the other detector. The energies of individual transitions were determined in singles runs. A linear sliding pulser was used to apply corrections for nonlinearity in the spectroscopy system.

Both high- and low-energy gamma rays were observed in singles and coincidence spectra and a decay scheme for the low-lying levels of $^{78}$Se was constructed. This decay scheme includes a previously

unreported transition of 194.5 keV between the 0+, 4+ doublet of states at 1500 keV and the second excited 2+ state at 1308 keV. This transition is of theoretical interest because it is within the so-called two phonon triplet of vibrational levels. An ambiguity in the placement of the 768 keV transition in previous radiative capture work was resolved by the placement of this transition between the 2328 keV and 1500 keV levels. The assignment of a 1010.4 keV transition to $^{78}$Se, as reported in earlier work, was not supported by the present data.

# CHAPTER I

## INTRODUCTION

The atomic nucleus remains one of the most challenging physical systems known despite sixty years of intensive investigation. There is no comprehensive microscopic theory of the nucleus (1), and only recently have various phenomenological nuclear models been shown to be fundamentally compatible (2). The acquisition not only of more nuclear data, but also of data of greater precision and reliability, is necessary to check theoretical predictions and to stimulate the development of improved theories of the nucleus.

The study of the gamma rays emitted in the radiative deexcitation of a nucleus is one important experimental method (3). The excited nucleus may be a product of radioactive decay or of various nuclear reactions. The present research uses the thermal neutron capture reaction to populate excited states of the nucleus $^{78}Se$, and information about the structure of this nucleus is obtained by observation of the gamma rays emitted in the decay of these excited states. Preliminary results on the reaction $^{77}Se(n, \gamma)^{78}Se$ have been previously reported (4).

### Radiative Capture and Nuclear Structure Studies

As recent reviews by Motz (5) and by Bergqvist and Starfelt (6) indicate, a wide variety of techniques and objectives are found

in radiative capture studies. Although increasing effort is being devoted to the understanding of neutron-nucleus reaction mechanisms (7) most effort is in the area of nuclear structure research. Bollinger (8) remarks: "Historically first and still consuming the most scientific effort, the $(n,\gamma)$ reaction is merely used as a way to populate low-energy nuclear states so as to obtain information about these states; thus, this area of work is very closely related to the conventional $\gamma$ and $\beta$ ray spectroscopy carried out with radioactive sources."

Thermal neutron capture is a useful method of populating excited nuclear states for two principal reasons. First, many isotopes can be formed by neutron capture which are not produced by radioactive decay. Second, thermal neutron capture populates a greater percentage of low-lying nuclear levels than do charged particle reactions. This is partly because the latter are usually direct reactions involving interaction of the projectile with specific single-particle states of the target nucleus. Selection rules thus limit the number of states which can be populated. The neutron capture-produced state generally decays through several cascades of gamma rays so that low-lying levels differing from the capture state by several units of angular momentum are observed. This encouraging picture is somewhat modified by the Porter-Thomas fluctuations, discussed in Chapter II, which may greatly weaken certain transitions. Other transitions, however, are strengthened, and the net result of these factors is that essentially all states below two MeV are populated by the thermal neutron capture reaction in medium and heavy nuclei.

A neutron capture gamma ray spectrum taken with a Ge(Li) detector typically shows three distinct regions: a high energy region with strong, well separated peaks, a medium energy region with a mass of unresolved transitions, and a low-energy region with generally resolvable peaks of differing intensity. The great number of transitions observed (often several hundred in heavy nuclei) makes good energy resolution in the detector of prime importance. For this reason thermal neutron capture gamma ray spectroscopy has been greatly facilitated by the development of the lithium-drifted germanium (Ge(Li)) detector (9). The good energy resolution, on the order of a few keV, and reasonable efficiency (up to 20 per cent of that of a 3 by 3 inch sodium iodide scintillator at 1.3 MeV) of the Ge(Li) diode have made it the detector of choice for most (n,$\gamma$) work.

Both the large number of gamma transitions observed and the complexity of the decay scheme of medium and heavy nuclei make gamma-gamma coincidence studies desirable for the unambiguous placement of transitions in a decay scheme. The work of Bolotin (10) and others has shown that the exclusive use of Ge(Li) detectors in (n,$\gamma$) coincidence studies is far preferable to the combination of a Ge(Li) and a scintillation detector, despite the greater efficiency of the latter.

The development of a radiative capture facility at the Georgia Tech Research Reactor was undertaken to complement existing radioisotope nuclear structure studies. The capture facility and instrumentation used for data acquisition are described in Chapter III, and the procedure for analyzing the data is given in Chapter IV.

## The Nucleus $^{78}_{34}Se_{44}$

One of the more important developments in the history of nuclear theory was the realization by Bohr, Mottelson, and Pines (11) that many nuclear properties could be understood if the nucleus were viewed as a many-body system exhibiting pairing correlations characteristic of superfluids. Subsequent work by Belyaev (12) and others has been reviewed by Nathan and Nilsson (13) and by Bohr and Mottelson (14). Although many difficulties remain the many-body approach stimulated by pairing theory seems to offer the best hope for a satisfactory theory of the nucleus. An experimental investigation which would contribute to the development of many-body nuclear theory was thus desirable.

Investigations by several authors (15,16 ) have shown that the energy gap in the single-particle spectrum of even-even nuclei, long thought to be due to pairing correlations alone, can also be obtained from self-consistent calculations without explicit correlations. Faessler et al. (17) studied theoretically the relative contributions of pairing and self-consistency to the energy gap in several nuclei including $^{78}Se$. Because no high-resolution coincidence study of radiative capture in $^{77}Se$ had been published, the study of the reaction $^{77}Se(n,\gamma)^{78}Se$ was chosen.

The level scheme of $^{78}Se$ has been previously investigated by radioactive decay (18,19 ), by Coulomb excitation (20), by (p,p) and (d,p) reactions (21,22,23)and by alpha particle stripping reactions on $^{76}Ge$ (24). Thermal neutron capture data were summarized by Bartholomew et al. (25). A decay scheme constructed from data up to 1966 was published by Artna (26).

A study by Rabenstein and Vonach (27), published while the present work was underway, gives Ge(Li) - Ge(Li) coincidence data for thermal neutron capture in natural selenium.

The present research was complementary to previous work in several respects. The radioactive decay studies populated only a small number of levels directly and were not expected to yield complete decay schemes. The Coulomb excitation work, as well as the earlier thermal capture studies, was hampered by detectors of low resolution and by low count rates. Weak or closely spaced peaks were thus likely not to have been observed. The thermal capture studies of Rabenstein and Vonach (27), although employing instrumentation comparable to that used in the present research, were hampered by the use of a natural target in place of a target isotopically enriched in $^{77}$Se. In natural selenium over 70 per cent of thermal neutron capture is in $^{76}$Se and the resulting decay of $^{77}$Se yields a very complex gamma ray spectrum. The task of separating peaks from $^{78}$Se decay from those in $^{77}$Se was quite likely to lead to ambiguities. Indeed, the paper of Rabenstein and Vonach contained several transitions placed twice in the decay scheme, indicating that further study with an enriched $^{77}$Se target was needed to properly place these transitions in the decay scheme.

The principal features of the level scheme of $^{78}$Se are a 2+ first excited state, a 0+, 2+, 4+ triplet of states at an energy roughly twice that of the first excited state, and enhanced E2 transition probability from the first excited state to the 0+ ground state. These features are characteristic of so-called vibrational nuclei,

since the level structure of the low-lying collective states is analogous to that of an anharmonic oscillator (28).

The data taken from radiative capture in $^{77}Se$ are presented in Chapter V. A level scheme based on these data and including previous information from other reactions is presented in Chapter VI. This level scheme is then discussed using the phenomenological anharmonic oscillator model. Conclusions and recommendations for further work are given in Chapter VII.

# CHAPTER II

## THE NEUTRON CAPTURE REACTION

Rather early in the history of experimental nuclear physics it was noticed that neutrons were very readily captured by some nuclei (29). This was attributed in part to the absence of Coulomb repulsion between a neutron and the positively charged nucleus, but the mechanism of capture was not then understood. Even today experimental and theoretical work is being done in an attempt to better understand the capture process (8).

### The Compound Nucleus

The first major contribution to an understanding of neutron capture was the formulation of the compound nucleus model by Niels Bohr. The essential hypothesis is stated in his first paper on the subject (31):

> Capture processes or neutrons are especially significant in offering a direct course of information about the mechanism of collision between the neutron and the nucleus. Indeed, the remarkable sharpness of the lines of the characteristic gamma-ray spectra of the radioactive elements proves that the lifetime of the excited nuclear states involved in the emission of such spectra is very much longer than the periods, circa $10^{-20}$ seconds, of these lines themselves. In order that the probability of emission of a similar radiation during a collision between a high-speed neutron and a nucleus shall be large enough to account for the experimental cross-sections for these capture processes, it is therefore clear that the duration of the encounter must be extremely long compared with the time interval, circa $10^{-21}$ sec., which the neutron would use in simply passing through a space region of nuclear dimensions.

> The phenomena of neutron capture thus force us to assume that a collision between a high-speed neutron and a heavy nucleus will in the first place result in the formation of a compound system of remarkable stability. The possible later breakup of this intermediate system by the ejection of a material particle, or its passing with emission of radiation to a final stable state, must in fact be considered as separate competing processes which have no immediate connection with the first stage of the encounter.

An obvious consequence of the compound nucleus hypothesis is that, since the energy of the incoming particle is very rapidly distributed among all the nucleons in the target nucleus, it is highly unlikely that enough energy will subsequently be concentrated on any one nucleon to allow it to escape. The cross-section for capture is thus enhanced relative to that for scattering.

The neutron capture cross-section as a function of energy shows two distinct regions in most nuclei (Figure 1). At the higher incident neutron energies peaks (resonances) are observed. Resonance neutron capture studies are conducted with neutron energies limited to include one, or a few, of these resonances. At very low neutron energies the tails of all the resonances overlap (32,33) to produce a large cross-section. Thermal neutron capture takes place at energies on the order of 0.025 eV.

In thermal neutron capture the excitation energy of the compound system is due to the binding energy of the captured neutron. This excited compound system, referred to as the capture state, is extremely complex, meaning that its wavefunction has a large number of nonzero components when expanded in single-particle basis states. Collective nuclear excitations such as the photonuclear giant resonance (33) are complex in this sense also, but the thermal neutron capture state appears to have no simple collective explanation.

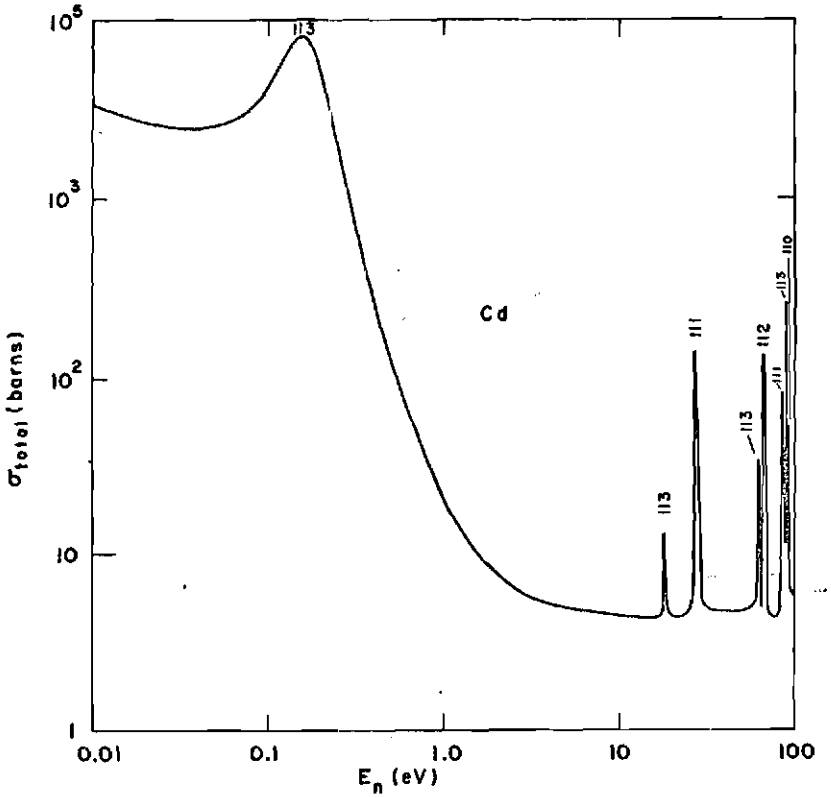


Figure 1. Total Neutron Cross-section for Natural Cadmium (30).

The complexity of the capture state has one important implication for radiative capture studies. Stated briefly, the probability of a transition from the capture state to a given final state (called a primary transition) depends not only on the energies, spins, and parities of the two states but also has large random fluctuations from one final state to the next. In practice this means that two adjacent low-lying levels with the same spin and parity may be populated by primary transitions having intensities differing by orders of magnitude.

The explanation for this large fluctuation in primary gamma-ray transition probabilities was first given by Porter and Thomas (34). Subsequent work by Wigner (35), Porter and Rosenzweig (36), and Mehta (37) led to an understanding of these Porter-Thomas fluctuations in terms of random matrices. A concise treatment has been given by Bohr and Mottelson (38) and is summarized here. The Hamiltonian of the compound system is represented by a matrix in which the individual matrix elements are assumed to have a random probability distribution. The matrix elements are assumed to be uncorrelated, except that they must satisfy the conditions imposed by physical symmetries (rotational and time-reversal invariance and Hermeticity of the Hamiltonian). They are also assumed to remain uncorrelated under an arbitrary unitary transformation of basis states (39). Then the ensemble of Hamiltonians with these matrix elements may be taken to be invariant to an orthogonal change of bases, and the joint distribution function (40) for the amplitudes

$C_i$ of the basis vectors in an expansion of the compound state is independent of the amplitudes:

$$P(C_1,C_2,\ldots,C_N) = 2/\Omega_N$$

where $\Omega_N$ is a normalization constant and N the dimensionality of the basis space. The sum of squares of the $C_i$ is constrained to be unity to preserve wavefunction normalization. For very large values of N, a reasonable assumption in medium-Z and heavy nuclei, it can be shown that the distribution function for a single amplitude is approximated by

$$P(C_1) = (N/2\pi)^{\frac{1}{2}}\exp(-\tfrac{1}{2}NC_1^2).$$

This distribution has the form of a chi-squared distribution with one degree of freedom (34). To apply this result to gamma emission from the compound capture state we need only note that the probability of transition from the capture state to a given final state is proportional to the probability $(C_1)^2$ of a single component in the compound state, since we may arbitrarily choose our basis set so that the final state is a basis vector. Then the form of the distribution $P(C_1)$, a broad exponential rather than a sharp peak, shows that $(C)^2$ can vary over a wide range. The most likely transition probability is in fact zero, but the tail of the distribution P(C) extends into observable amplitudes. Experimental results from a wide range of nuclei have been fitted well by the Porter-Thomas distribution.

In spite of the fact that primary transitions do not populate all the low-lying energy levels directly, virtually all low-lying levels are observed in radiative capture studies. These levels are populated via cascade gamma rays (secondary transitions) involving a large number of intermediate energy levels.

There is growing evidence that in a few nuclei direct capture mechanisms as well as the compound nucleus reaction play a role. Reviews by Bollinger (8) and by Bergqvist and Starfelt (6) summarize the existing data on the neutron capture reaction.

## Gamma Emission From the Capture State

In Chapter V, on the thermal neutron capture reaction in selenium-77, it is assumed that any gamma transition with an energy greater than 75 per cent of the neutron binding energy is a primary transition. The reasoning supporting this empirical rule is as follows. First, a simple single-particle model for gamma emission (33) gives a transition probability proportional to $E^{2\lambda+1}$, where E is the energy difference between initial and final states and $\lambda$ is the multipolarity of the transition. This favors high energy transitions. There is also an inverse dependence on the density of final states which favors low energy transitions, but for medium-Z and heavy nuclei the $E^{2\lambda+1}$-dependence predominates (41). The high-lying capture state has a strong tendency to decay to low-lying states, then, and higher-lying levels will be populated by transitions of very low intensity. Any high-energy transition from a level other than the capture state would therefore be unobservable. Many radiative capture studies have

borne out this prediction for both thermal and resonance neutron capture, so that the rule may be used with confidence.

A second property of the radiative capture reaction is that only states having spin and parity within a limited range are populated directly by primary transitions. Because of the low energy of thermal neutrons, capture is essentially s-wave capture. This implies that the spin of the capture state is $I \pm \frac{1}{2}$, where I is the spin of the ground state of the target nucleus and the neutron has spin $\frac{1}{2}$. The parity of the capture state is the same as that of the target (42). Selenium-77 has a ground state with spin and parity $\frac{1}{2}$-. The capture state in $^{78}Se$ is then known to be either 0- or 1-. Very strong primary transitions are usually E1 (41), and the spins of states they populate may be limited to a small range. Again in the case of $^{78}Se$ the spin of a level populated by a strong primary which is assumed to be E1 is limited to the range (0,1,2). E1 radiation involves a parity change between the initial and the final state so that the low-lying level must have even parity if the transition is indeed E1. Weaker primary transitions do not allow the limitation of final-state spin and parity to this small range since Porter-Thomas fluctuations may enhance normally weak M1 or E2 transitions. Resonance and average-resonance capture studies allow more certainty in spin and parity determination, as discussed by Bollinger (41).

# CHAPTER III

## EXPERIMENTAL APPARATUS

The purpose of the work was to measure, as accurately as possible, the energy and intensity of gamma-rays from various excited states and to correlate those radiations that were emitted in cascades. The decision to use Ge(Li) detectors exclusively for the radiative capture experiments reported here imposed several stringent requirements on the experimental apparatus. Coincidence experiments were more easily performed with an external target facility, requiring a neutron beam extraction and collimation system. The beam could contain no appreciable fast neutron flux, in order to avoid damage to the detector crystals and in order to restrict capture to s-wave capture for spin limitation (as discussed in Chapter II). Because of low detector efficiency a high thermal neutron flux was desirable. For this reason the Georgia Tech Research Reactor was employed as the neutron source.

Two types of experimental runs were to be made. Singles runs, for precise gamma ray energy determination, employed only one of the detectors and required signal-processing instrumentation which preserved the inherently high resolution of the Ge(Li) detectors. Coincidence runs for identification of cascade relationships employed both detectors and required a fast-slow coincidence system (43) which did not degrade the detector resolution at high singles count rates;

in order to handle anticipated count rates of up to 50,000 counts per second the circuitry had to be able to compensate for pulse pileup distortion (44) and baseline shifts. Finally, despite the high singles data rates, the coincidence event rate was expected to be only on the order of 100 counts per minute and a multiparameter data acquisition system was necessary to avoid prohibitively long collection times.

The apparatus used in the experiments discussed in this thesis may be conveniently separated into three groups: The reactor beam port, the target and detectors, and the electronic instrumentation. This grouping is meaningful not only physically but also functionally. The beam port can be viewed as a hole which emitted a filtered, collimated thermal neutron beam; this beam entered the target and detectors, the output of which was two preamplifier output signals; finally these signals entered the electronic instrumentation and emerged as digital data on magnetic tape. In a sense the computer programs which reduced the data off-line could be considered a part of the apparatus, but they are discussed in the chapter on procedure.

## The Reactor Beam Port

The term port is here used to refer not only to the physical port, or opening in the reactor shielding, but also to the internal configuration of the tangential tube and plug necessary to extract, collimate, and filter the neutron beam. The physical port used at the Georgia Tech Research Reactor was designated H-12 and was part of a tangential through tube, meaning that it passed completely through the reactor shielding from one face to the other and was tangential to

the core rather than pointing directly toward the core (Figure 2). With the reactor operating at a thermal power level of one megawatt a total neutron flux of $2 \times 10^{13}$ $n/cm^2$-sec was measured at the midpoint of the tube (45). A graphite "blanket" two feet thick surrounded the core and served to moderate the neutrons coming from the core, also scattering some of them into the tangential through tubes. A graphite scattering block 12" long and 6" in diameter was located inside the through tube between two graphite cylinders. These cylinders, each four feet long with a 3/4 inch center hole, were in contact with the plugs which close each end of the through tube. Neutrons scattered toward the target from the graphite scattering block were reflected through an angle greater than 90 degrees, increasing the relative proportion of low-energy neutrons entering the collimator.

The removable experimental plug containing the collimator and beam filter was constructed of steel and dense concrete (Figure 3). This plug was stepped near its inner end so that there was no straight-line path for neutrons to follow which did not pass through dense concrete shielding. At its inner end the plug was faced with a 1/4 inch Boral plate with a 1/2 inch diameter center hole. Boral, containing 9 percent boron, was an effective absorber of thermal neutrons. Lead, concrete, and steel shielding behind this plate absorbed gamma rays emitted in neutron capture.

The major part of the collimator was constructed inside the three inch I.D. outer part of the plug, as depicted in Figure 2. Discs of borated polyethylene, one inch thick by 1/2 inch I.D., were

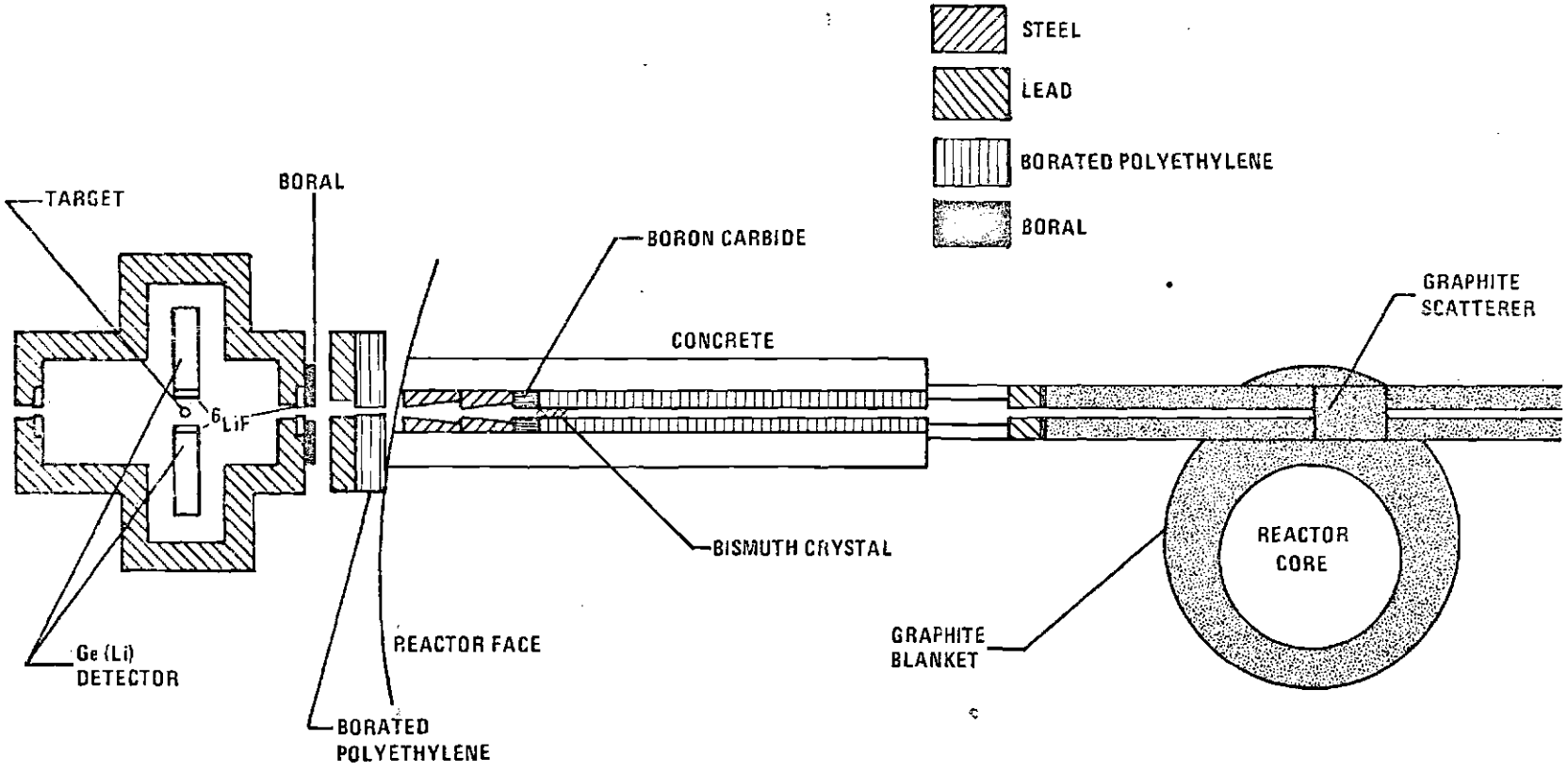


Figure 2. Reactor Beam Port (Not to Scale).

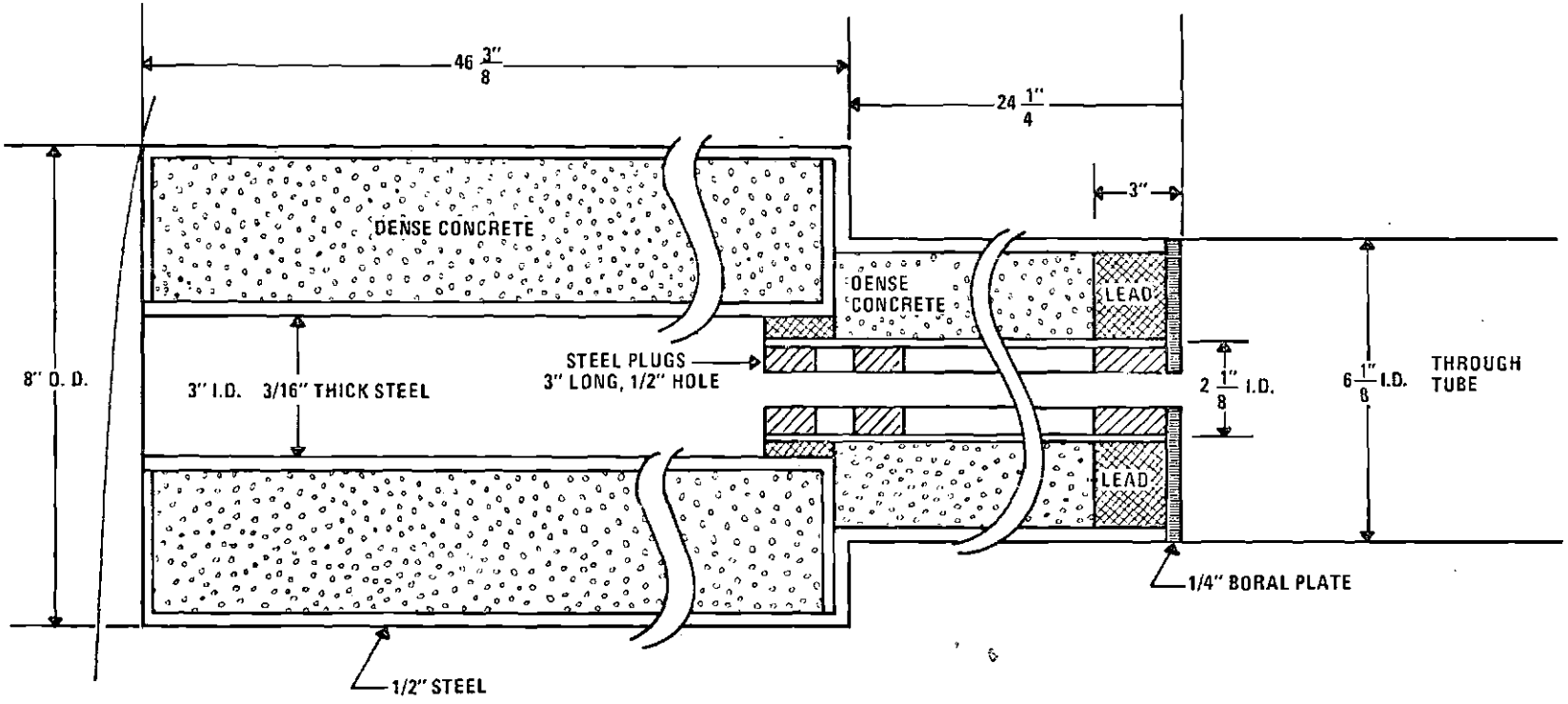


Figure 3. Experimental Plug Details.

stacked inside the plug for a distance of 32 inches. The carbon and hydrogen in the polyethylene served to moderate neutrons outside the desired beam and the boron captured the moderated neutrons. These discs were followed by a three inch long by 3/4 inch I.D. cylinder of boron carbide cast in acrylic resin. The extremely high boron content of this material captured essentially all the thermal neutrons not stopped in the borated polyethylene. Gamma rays resulting from capture in boron were stopped by four steel plugs, each four inches long. These plugs had a center hole tapering from 1/2 inch I.D. at the outer end to 3/4 inch I.D. at the inner end. The taper prevented the target and detectors from seeing an appreciable amount of steel; neutron capture in iron yielded gamma rays which would have increased the background count rate.

The beam was filtered by a bismuth single crystal 1/2 inch in diameter by five inches long located inside the outer-most borated polyethylene discs. Bismuth had a high absorption cross-section for photons and a high scattering cross section for fast neutrons but a relatively low scattering and absorption cross-section for thermal neutrons. The undesired gammas and fast neutrons were thus preferentially removed from the beam. Since bismuth did attenuate the thermal neutron flux both by incoherent scattering and by coherent Bragg scattering several compromises were involved in the design of a beam filter. Clearly if a very "clean" beam, one low in gamma rays and fast neutrons, were desired a long bismuth filter must be used. This would also have reduced the transmitted thermal neutron flux. The original beam filter for the $(n,\gamma)$ studies consisted of one two inch

and one five inch bismuth crystal. After several preliminary runs it was decided that a higher thermal flux was needed and that more gammas and fast neutrons could be tolerated, so the two inch crystal was removed. With both crystals in the beam a thermal flux of $2 \times 10^6$ $n/cm^2$-sec and a cadmium ratio of 150 were measured at the outer end of the experimental plug. Flux measurements were made by measuring the activation of known masses of gold foil. With the five-inch crystal alone a flux of $3 \times 10^6$ $n/cm^2$-sec was estimated on the basis of the increase in the singles count rate. The cadmium ratio, proportional to the ratio of thermal neutrons to fast neutrons in the beam, is so called because cadmium is used to filter out neutrons with energies below the Cd resonance (see Figure 1).

The contribution to the thermal neutron attenuation in bismuth from Bragg scattering in the crystal lattice made a single crystal preferable to a polycrystalline cast bismuth filter; however, other thermal capture facilities (46) have successfully used large cast bismuth filters located inside the graphite moderator. Some improvement in thermal flux could have been obtained by varying the crystal orientation, but this was not considered worth the additional expense and experimental complication.

The bismuth crystal was encased in a thin-walled aluminum tube which fitted inside a set of borated polyethylene discs with enlarged center holes. The aluminum container avoided possible problems with contamination of the experimental facility by activation products of bismuth.

It was found that detectable fluxes of fast neutrons and gammas were present at the outer end of the experimental plug, presumably due to leakage through the spaces between the borated polyethylene discs and the plug. Two sheets of borated polyethylene, two feet square by one inch thick, were placed against the plug end with a 3/4 inch diameter hole through them for passage of the beam. A two inch layer of lead brick outside this final neutron shielding absorbed gamma rays. This extra shielding had the additional advantage that it reduced the number of neutrons scattered into the reactor experimental area, lowering the background seen by nearby neutron diffractometers. A small disc of $^{6}$Li-enriched LiF was inserted into the beam hole in the lead layer to act as a shutter.

## The Target and Detectors

Since the reactor experimental area had a moderately high ambient flux of gamma radiation the target and detectors were enclosed in a shield, referred to as a "cave", made from 8"x4"x2" lead brick. This cave was supported on a steel and aluminum table which in turn rested on four screw jacks. The table could be leveled, raised, or lowered by adjustment of the jacks so that the target and detectors were positioned properly with respect to the fixed neutron beam. The top of the table as well as a center supporting beam were of aluminum. This material was chosen so that subsequent angular correlation experiments could be more easily performed: aluminum, being nonmagnetic, does not introduce perturbations into the magnetic fields inside movable photomultiplier tubes.

Neutron capture in lead yields energetic gamma rays; the cave was designed to minimize the possibility of having thermal neutrons strike its walls. The beam entered the front of the cave through a 3/4 inch hole in a lead brick. This brick was shielded by a three inch diameter by 1/2 inch thick disc of $^{6}$Li-enriched LiF cast in acrylic resin. Rather than being stopped inside the cave after it had passed through the target the beam was allowed to leave through another 3/4" hole in the rear wall. This hole was also faced with $^{6}$LiF.

The beam was finally absorbed by a beam catcher located approximately 2 feet behind the rear wall of the cave. The beam catcher consisted of a paraffin and borax cylinder which stopped the neutrons and an outer shield of 2" thick cast lead and lead shot to absorb gammas. The catcher was contained in a steel drum and supported on a welded steel stand at the proper height so that the beam entered through a 2" diameter hole in the front lead shielding.

The selenium targets were encapsulated in thin-walled aluminum containers, aluminum being used because of its relatively low capture cross section. The targets were supported in the beam in an aluminum foil sling suspended from a plastic holder which rested on the floor of the cave. This minimized the amount of aluminum in the beam.

The two detectors used in the present study were lithium-drifted germanium diodes. The larger was a trapezoidal detector of 30cc active volume and resolution 3.7 keV Full Width at Half Maximum (FWHM) at 1.33 MeV, manufactured by Nuclear Diodes Corporation.

The smaller detector was a 10cc trapezoidal crystal with a resolution of 4.5 keV (FWHM) at 1.33 MeV fabricated by the Department of Physics, Emory University. Both detectors were mounted in right-angle cryostats which extended downward through holes in the table into liquid nitrogen dewars. The center of each detector was made level with the beam by small aluminum and wooden shims under the horizontal part of the cryostat. The detectors faced each other at right angles to the beam. To prevent neutron damage in the detectors a disc of $^{6}$Li-enriched LiF cast in acrylic resin was placed over the entrance window of each detector.

## The Electronic Instrumentation

The electronic instrumentation (Figure 4) may be conveniently divided into four subgroups: the linear signal-processing system, the fast timing system, the digital multiparameter magnetic tape system, and the spectrum stabilization system.

The linear signal-processing modules were built at the Georgia Institute of Technology from designs supplied by the Argonne National Laboratory Electronics Group (44). There were two arms in the system, each arm providing one parameter for two-parameter coincidence studies. An arm consisted of a detector, a preamplifier, a Linear Pulse Amplifier (LPA), a Linear Pulse Selector (LPS), and a Linear Gate and Stretcher (LGS). The detectors provided a current pulse whose area was directly proportional to the energy given up in the detector crystal by the incident photon. The preamplifiers converted this current pulse into a voltage pulse (see the upper signal in Figure 5) whose amplitude was linearly proportional to the photon energy. On the 10cc

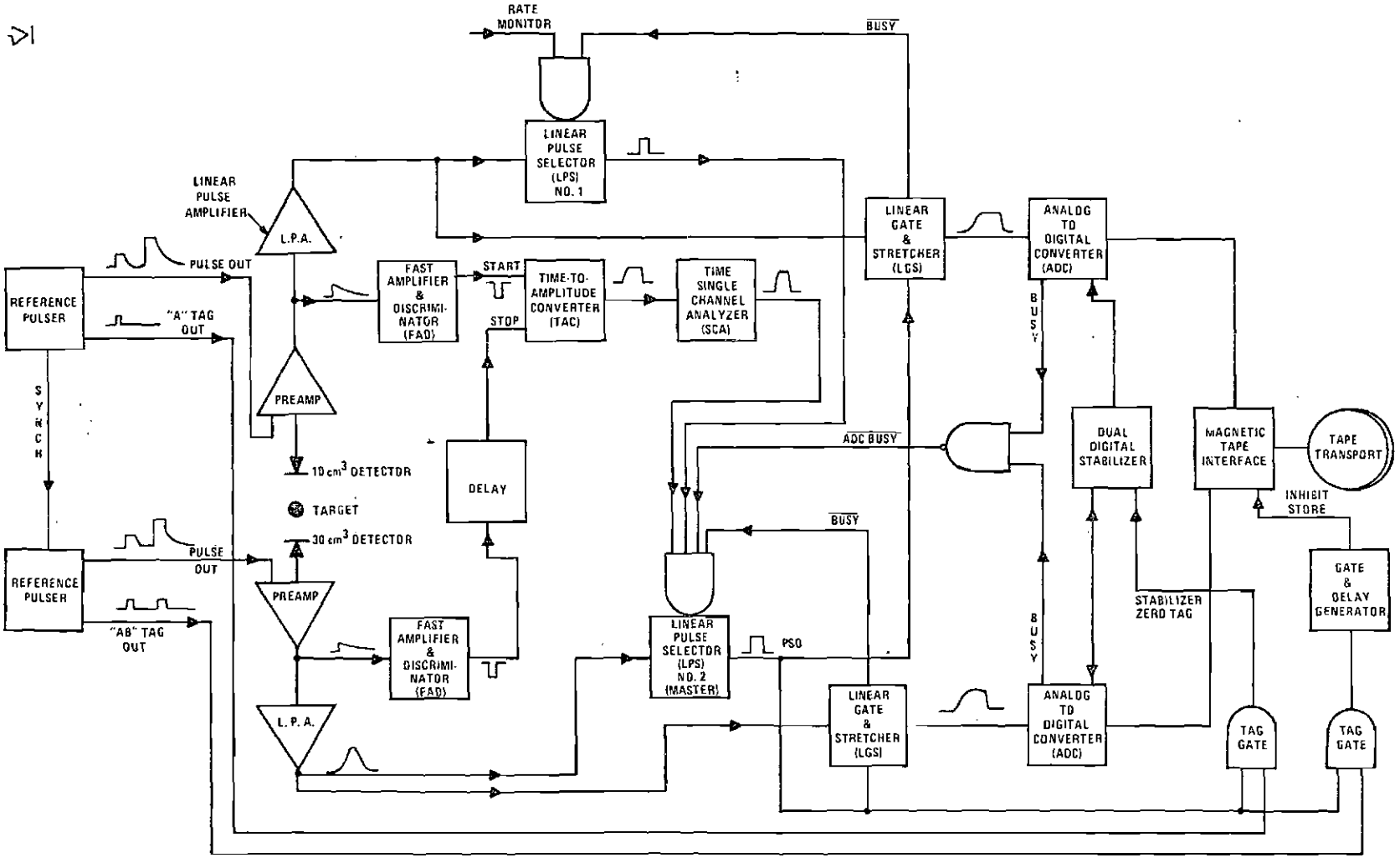


Figure 4. Electronic Instrumentation Block Diagram.

detector a Tennelec, Inc. TC-135 preamplifier was used, and that used on the 30cc detector was an integrally mounted Nuclear Diodes ND-101. The LPA design used single-RC pulse shaping (47) with differentation and integration time constants adjustable to meet experimental conditions. The output pulse shape is shown in Figure 5; the slow risetime gives a better signal-to-noise ratio than faster shaping. For the experiments reported here a time constant of two microseconds was empirically found to give the best resolution at moderately high count rates (on the order of 10,000 counts per second). Baseline restoration was included in the amplifier as well as in the LPS and LGS to improve high count rate performance and to filter out low-frequency noise.

Following the LPA was a module referred to as the Linear Pulse Selector (LPS). It contained a single-channel analyzer, a pulse shape discriminator, and a gating circuit which combined several logic signals and generated an output called PSO. Only when an LGS received a PSO signal at its control input did it open its linear gate and allow a pulse to be analyzed. Inputs to the LPS gating circuit came from the single-channel alalyzer and pulse shape discriminator circuits in the LPS and from up to five external gating signals, as shown in Figure 4. An adjustable delay was included in the LPS so that the PSO signal from one LPS could be used as a gate input to another LPS. This was done in the coincidence studies reported here; Figure 5 illustrates that the output from LPS no. 1 occurred before that from LPS no. 2. The second LPS was referred to as the master LPS, since its PSO output controlled both LGS modules.

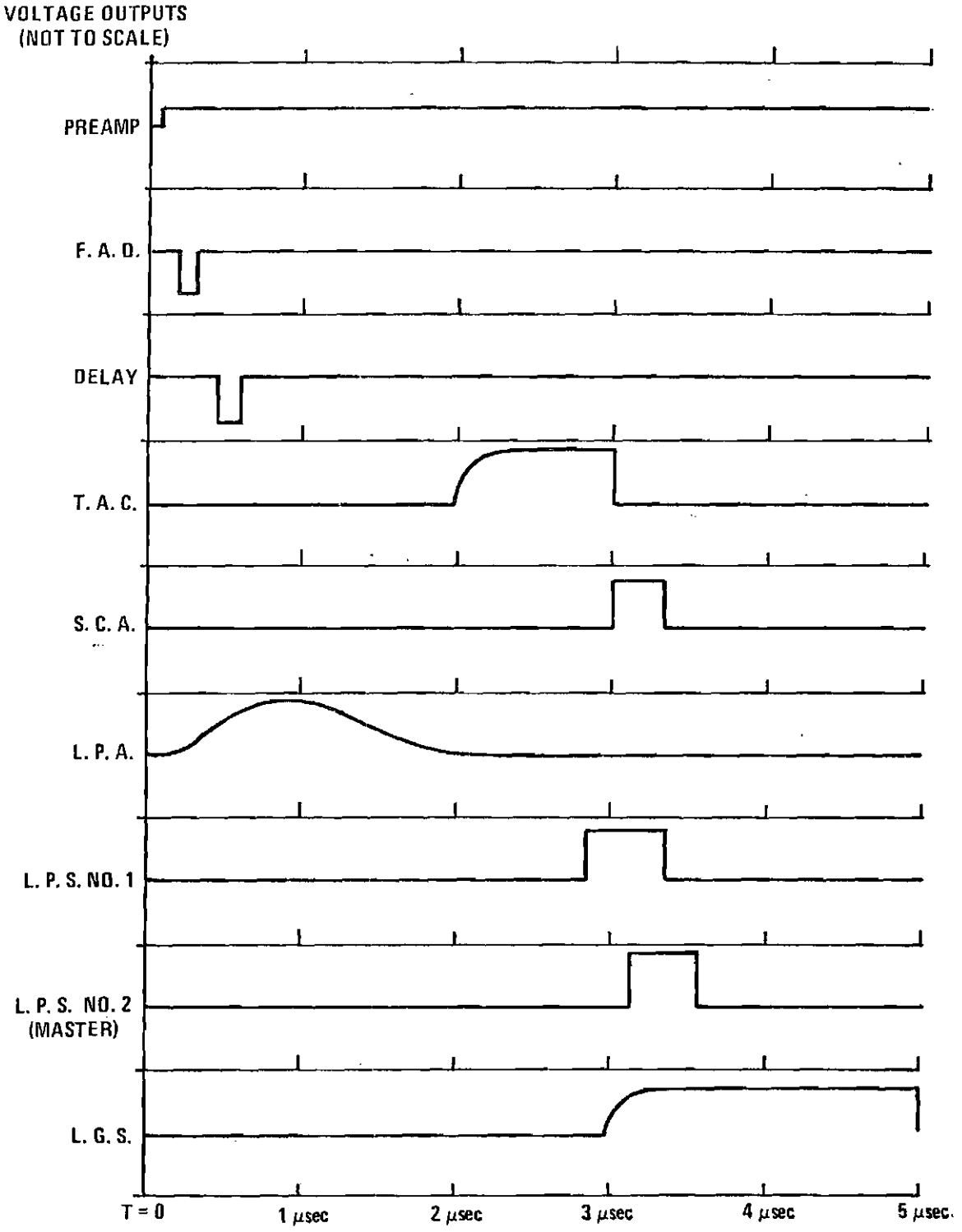


Figure 5. Timing Relationships of Signals (Horizontal Axis is Approximate Only).

A pulse shape discriminator was included in the LPS to reduce the degradation of system resolution by pulse pileup at high count rates. There are two types of pulse pileup. Tail pileup is a term denoting the occurrence of two pulses close together in time so that one pulse rides on the exponential tail of the other. It was undesirable to analyze such pulses because the amplitude information in the second pulse was distorted. To prevent tail pileup the LPS remained dead for a time equal to three pulse widths; no pulse was analyzed until the preceding pulse had decayed to negligible amplitude. Another type of pileup is referred to as peak pileup: Two pulses occur so close together that their peaks overlap. This was rejected in the LPS by a pulse shape discrimination circuit which essentially measured the risetime of the incoming pulse and generated a logic signal only when this risetime was within very narrow predetermined limits. Because a pulse composed of two nearly coincident overlapping pulses generally had a distorted leading edge, this risetime discrimination circuit effectively eliminated peak pileup distortion.

The final module in the linear signal-processing system was the Linear Gate and Stretcher (LGS). It had two inputs, as shown in Figure 4: The signal from the LPA entered a linear input and the PSO output of the master LPS entered a control input. Thus, although the decision as to whether a signal was to be analyzed was made in the LPS, it was not until the pulse reached the linear gate and found it closed that actual rejection occurred. The LGS contained a biased amplifier which subtracted a fixed voltage from the amplitude of each incoming pulse. This bias adjustment allowed an energy region of interest to be expanded

in the Analog-to-Digital Converter (ADC) and avoided having to digitize unwanted portions of the spectrum. Finally a stretcher in the LGS generated a very wide (five to ten microseconds) output pulse, shown at the bottom of Figure 5, for input to the ADC.

The purpose of the fast timing system was to determine whether gamma rays entered the two detectors in coincidence - i.e., within a certain specified time of each other. The time of occurrence of an event in a detector was determined by an Elron, Inc. FAD-N-1 Fast Amplifier and Discriminator (FAD). This module generated an output pulse whenever the preamplifier output signal exceeded a threshold. Since this threshold was very low the timing relationship between the input and output signals of the FAD was essentially independent of the energy of the gamma ray. The output of one discriminator was fed into the "start" input of an Elron, Inc. TAC-N-1 Time-to-Amplitude-Converter (TAC) and the output of the other discriminator was delayed in a length of coaxial cable before entering the "stop" input of the TAC; Figure 5 shows the prompt and delayed FAD outputs. The TAC produced an output pulse whose amplitude was proportional to the time interval between its start and stop inputs. Thus the pulse amplitude spectrum from the TAC (Figure 6) represented the distribution of time intervals between detector pulses. The fixed delay served to shift the origin of the time spectrum so that truly simultaneous events appeared at some nonzero output pulse amplitude ($t_o$ in Figure 6). The time Single Channel Analyzer (SCA) looked at the TAC output with its acceptance window, shown in Figure 6, set to include that portion of the time spectrum which represented true coincidences.

As one of its external gating inputs, the master LPS received the time SCA output which indicated that a coincident pair of detector outputs (called an event) had occurred. If all the other LPS gate inputs, shown in Figure 4, were true this allowed the master LPS to open the LGS gates and permit the two pulses - one propagating down each arm of the system - to be analyzed.

In order to reduce dead time in the TAC it was desirable to have the stop input pulse rate higher than the start input rate. For this reason the larger, 30cc, detector fed the "stop" input. The time of occurrence of the TAC output pulse was determined by the time of arrival of the stop input. This TAC output pulse then determined the timing of the time SCA output, which (as shown in Figure 5) was required to overlap the other gating signals at the master LPS. If the master LPS was in the arm of the system fed by the larger detector, then, a more stable timing relationship among the signals arriving at its gating input was achieved.

Figure 6 illustrates the time spectrum obtained by having a conventional pulse height analyzer look at the TAC output pulses. The timing window on the SCA was set to accept a range of TAC output pulse amplitudes corresponding to a coincidence resolving time of about 100 nanoseconds for the experiments reported here. The advantage of using a TAC and SCA rather than a less expensive overlap coincidence circuit is illustrated here: The trapezoidal detectors used had rather large and variable output pulse risetimes compared to scintillators or coaxial semiconductor detectors. With the TAC the time spectrum could be examined visually and a very good determination made of the best

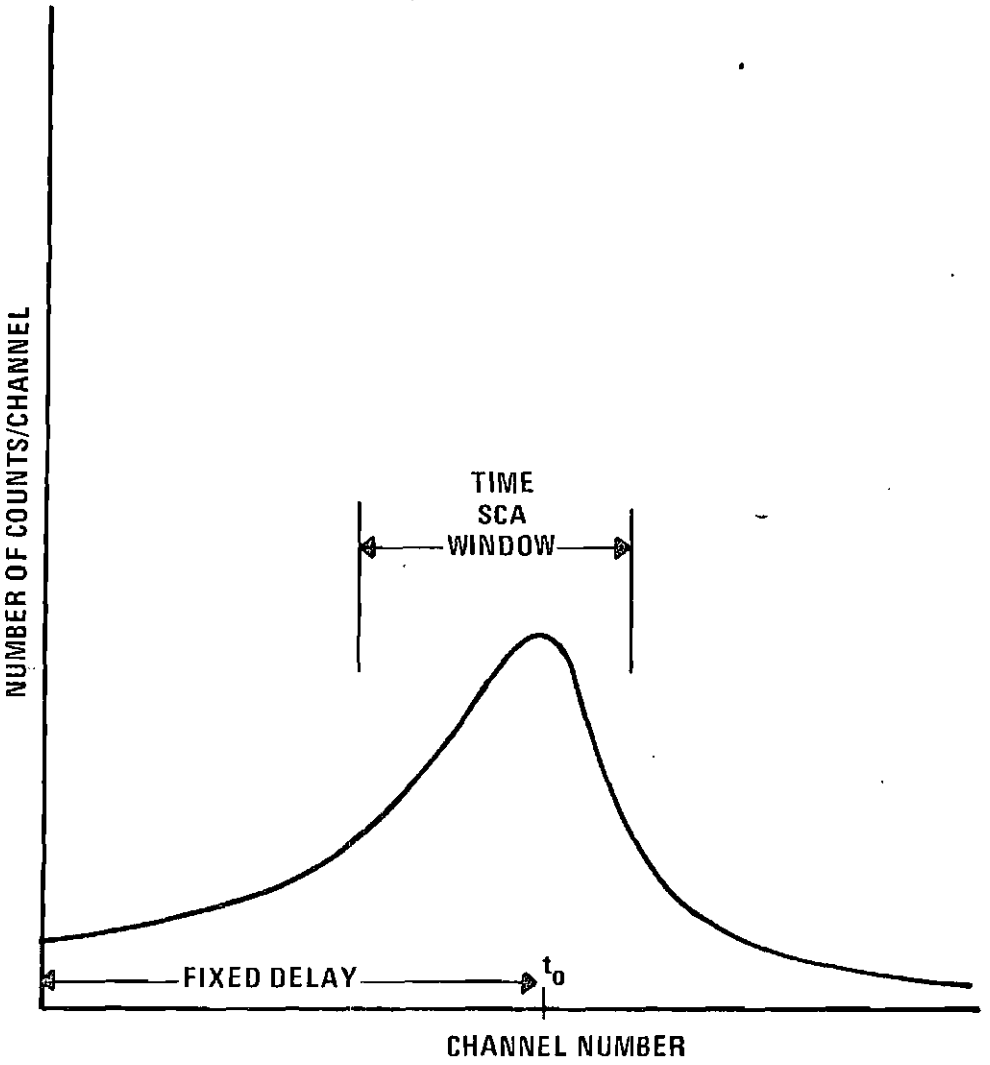


Figure 6. Time Spectrum.

setting of the time window. This window setting could then be checked by using the SCA to gate the analyzer. (If desired, a third ADC could be added to the system and the time spectrum recorded with the pulse heights in a three-parameter arrangement, allowing lifetime studies on metastable excited states.)

The two preceding subgroups served to amplify, reshape, and inspect the outputs of the Ge(Li) detectors, and to produce outputs from the Linear Gate and Stretcher modules only if all the requisite coincidence, amplitude, and pulse shape conditions were satisfied. The remaining task was the conversion of the gamma energy information represented by the pulse amplitudes into digital form and the storage of this information on magnetic tape for subsequent analysis. The conversion was performed by two commercial analog-to-digital converters (Northern Scientific Company model NS-628) of the Wilkinson type having an oscillator frequency of 60 megahertz and 13 bit (8192 channel) resolution. In the experiments reported here the negative outputs of the LGS modules were fed into the ADC direct inputs in order to bypass redundant amplifier and stretcher stages in the ADC's.

The ADC outputs were two 13-bit addresses, busy signals, and "conversion complete" signals. These signals entered an interface which controlled both the ADC's and the magnetic tape transport. The interface, constructed with plug-in logic modules (Digital Equipment Corporation), allowed recording of one, two, or three 12-bit words per event. Each word was composed of bits selected by front-panel patchcords and could include data both from ADC's and from independently set flag registers. The number of words per event as well as the

length of a tape record (a block of data between inter-record gaps) were switch selectable. The LGS modules, the ADC's, and the interface produced busy signals whenever they were occupied in the processing of a pulse; these signals gated off the master LPS until another event could be analyzed.

The tape transport was a commercial incremental digital recorder (Cipher Data Products Model 100) with a maximum data recording rate of 1,000 six-bit frames, or 500 12-bit words, per second. Hence in two-parameter operation the maximum coincidence rate that could be handled by the system without loss of data was 250 events per second. Data were recorded in standard IBM compatible format at a density of 556 frames per inch.

The only major part of the instrumentation not yet discussed is the spectrum stabilization system. Since runs lasting several days were often required, any drift in either the zero level or the gain of the system would have resulted in distortion and degradation of the spectra. Consequently a digital servo stabilization system was employed. Reference peaks for the stabilizer were provided by two highly stable reference pulsers, one in each arm of the system. One peak was placed at the extreme lower end of each spectrum for zero stabilization and another at the upper end for gain stabilization. The pulser outputs, consisting of alternating high- and low-amplitude pulses, were injected at the input of each preamplifier to simulate detector signals. Since reference pulses and detector pulses entered the system together, it was desirable to label the reference pulses with "tag" pulses, produced by the reference pulsers simultaneously with the reference pulses (see Figure 4).

The stabilizer was a dual 4096 channel unit (Northern Scientific Company NS-404) which adjusted the gain and zero level of each ADC to compensate for drift. The operation of the zero and gain stabilization loops was slightly different. A low-amplitude reference pulse from the pulsers was accompanied by an "A" tag which informed the stabilizer that the accompanying pulse was a zero reference pulse. The stabilizer examined the digitized pulse amplitude and adjusted the ADC zero level to keep the reference peak within a preset window. The gain stabilizer, on the other hand, did not use a tag pulse. A digital window was set to include the upper reference peak from the pulser and any pulse falling within the upper half of this window caused the ADC conversion gain to be reduced. Conversely, pulses falling within the lower window half increased the conversion gain.

The gain stabilization loop was more effective when the reference pulser rate was several times as great as the experimental data rate within the gain window. A tag, called the "AB" tag in Figure 4, accompanied both zero and gain pulser outputs and caused the magnetic tape interface to reject (i.e., not store) the reference pulses. The time required to digitize a pulse was much less than that required to write it on tape; this allowed the reference pulsers to run at a sufficiently high rate to give good stabilization without introducing undue system dead time.

# CHAPTER IV

## DATA ANALYSIS PROCEDURE

The collection and analysis of data from the (n,γ) experiments were divided into two distinct phases. Singles spectra were taken to determine the energies and intensities of individual gamma transitions, and coincidence runs were then used to help place the transitions in a decay scheme.

### Singles Spectra and Gamma Energy Determination

The term singles spectra is used because these spectra were made using only one detector, with no coincidence requirement imposed. In place of the ADC and magnetic tape recording system which was used for the coincidence runs, a Northern Scientific Company NS-600 multichannel analyzer (MCA) received the Linear Gate and Stretcher (LGS in Figure 4) output and stored the spectrum in its 2048-channel memory. The spectra were recorded on punched paper tape and later converted to magnetic tape by a digital computer.

The precise determination of gamma energies required correcting for system nonlinearity using a technique sometimes referred to as the ramper method (48). Three spectra were required: the singles spectrum from the isotope under study, a calibration spectrum containing peaks of precisely known energy, and a correction spectrum. The correction spectrum was obtained by disconnecting the detector from the preamplifier, substituting an equivalent dummy capacitance, and applying

pulses from a very linear sliding pulser to the preamplifier test input. The sliding pulser (Berkeley Nucleonics GL-3) output was a train of pulses whose amplitudes slowly and uniformly increase with time to a maximum, then decrease at the same rate to zero. This cycle was repeated with a period of 50 seconds until sufficient counts were present in each channel of the MCA to make statistical fluctuations neglegible. If the system were completely linear the resulting correction spectrum would have been a straight horizontal line, the sliding pulser being specified as linear to within 0.025 per cent. Nonlinearities were recorded as deviations from this horizontal line. Finally the correction spectrum and the channel numbers of the centroids of the calibration and unknown peaks, together with the calibration peak energies, were supplied to a computer program (RAMPCL) which was developed at Argonne National Laboratory. This program determined the energies of the unknown peaks by the formula

$$E_s = E_{c1} + \left( \sum_{i=c1}^{s} R_i \right) \left( E_{c2} - E_{c1} \right) / \left( \sum_{i=c1}^{c2} R_i \right)$$

where $E_s$ is the energy of the unknown peak, $E_{c1}$ the lower calibration energy, $E_{c2}$ the upper calibration energy, c1 and c2 the centroids of the lower and upper calibration peaks, respectively, s the centroid of the unknown peak, and $R_i$ the contents of the ith channel of the correction spectrum. At each point in the spectrum, then, an accurate nonlinearity correction was made. This contrasts with other correction techniques (49) in which the correction is exact at only a few points.

The peak centroids were obtained by least-squares fitting of gaussian curves to the experimental data points. A computer program (GAUSS) developed at Argonne National Laboratory accepted a visually determined estimate of the background underlying the peaks and initial guesses at the peak centroids. The program subtracted the background continuum from the region and then varied the centroids, areas, and widths of the one or more gaussians until the sum of squares of the deviations of the experimental data points from the calculated curve was a minimum. GAUSS used an algorithm developed by W. C. Davidon (50) which converged to the best fit in a finite number of steps (given reasonably good initial guesses) and was considerably more efficient than steepest-descent fitting methods. The algorithm has been generalized by Stewart (51) and an exposition given by Fletcher and Powell (52).

Output from GAUSS consisted of the centroids, areas, and widths of the peaks together with a value of $\chi^2$, which is defined as the sum of squares of deviations divided by $\nu$, the number of degrees of freedom of the fit. $\nu$ is equal to the number of points in the region less three times the number of peaks being fitted to the region. Theoretically, a value of unity for $\chi^2$ is expected from statistical fluctuations in the data alone. Higher values indicate improper shape or location of the fitting peaks. For well-isolated peaks in the present work, $\chi^2$ ranged from 1 to 5. Badly shaped peaks or an attempt to fit several overlapping peaks to a region yielded higher values of $\chi^2$. The gaussian curves used were not skewed to simulate tails in the detector peaks although the peaks did show definite low-energy tailing.

The more accurately determined the energies of individual gamma transitions the more unambiguously they may be placed in a decay scheme. It has been found (48) that careful application of this method of energy determination can yield peak energies accurate to within 0.1 keV. The present studies gave somewhat worse (0.5-1.0 keV) agreement with accepted energy values. This was attributed to shifts in gain and zero level of the system between the calibration spectra and the unknown spectra; servo stabilization of these system parameters was not feasible with the MCA used.

## Coincidence Spectra

The placement of gamma transitions in decay schemes can in principle be made solely on the basis of energy and intensity balances and, indeed, valuable results have been obtained thereby (53). In practice, however, ambiguities arise due to errors in gamma ray energy determination and failure to resolve closely spaced multiplets. Coincidence experiments are thus needed to clearly and unambiguously establish cascade relationships.

The magnetic tape multiparameter analysis system described in the previous chapter was used to collect coincidence data from the (n,Y) reaction. Data were stored on magnetic tape in the form of events, each consisting of two twelve-bit words. One word of each event represented the gamma energy deposited in the 10cc detector; the other represented the energy deposited in the 30cc detector. A computer program (MULTI) developed by the author sorted the events into spectra representing those events in one detector which occurred in coincidence with events of a given energy in the other detector.

This energy selection was accomplished by specifying to MULTI the upper and lower channel numbers of a digital window. Thus the program simulated a conventional single-channel analyzer fast-slow coincidence system (43) gating a multichannel pulse-height analyzer. The entire energy range of both detectors was recorded on tape, thus several windows could be set and several corresponding spectra accumulated simultaneously. For 4096 by 4096 channel data acquisition, twelve spectra were accumulated for each pass of the data tape through MULTI. Repeated passes allowed accumulation of up to thirty coincidence spectra. In practice eight to ten reels of data were needed to obtain satisfactory statistics, each reel containing about $3 \times 10^6$ two-word events.

One problem in gamma-gamma coincidence work was that the Compton background underlying a peak may have been of comparable amplitude to the peak itself. When an energy window was set to include the peak, the underlying portion of the Compton background was included, and coincidences with the transitions giving rise to the background appeared to be in coincidence with the peak (43). A correction for this Compton coincidence was made by setting near the peak a window which included only background (Figure 7). If the peak and background windows were of equal width and the background were a horizontal line, subtraction of the spectrum in coincidence with the background window from that in coincidence with the peak window would yield a "true" coincidence spectrum. The width and position of the background window was adjusted empirically to compensate for nonuniformity of the background.

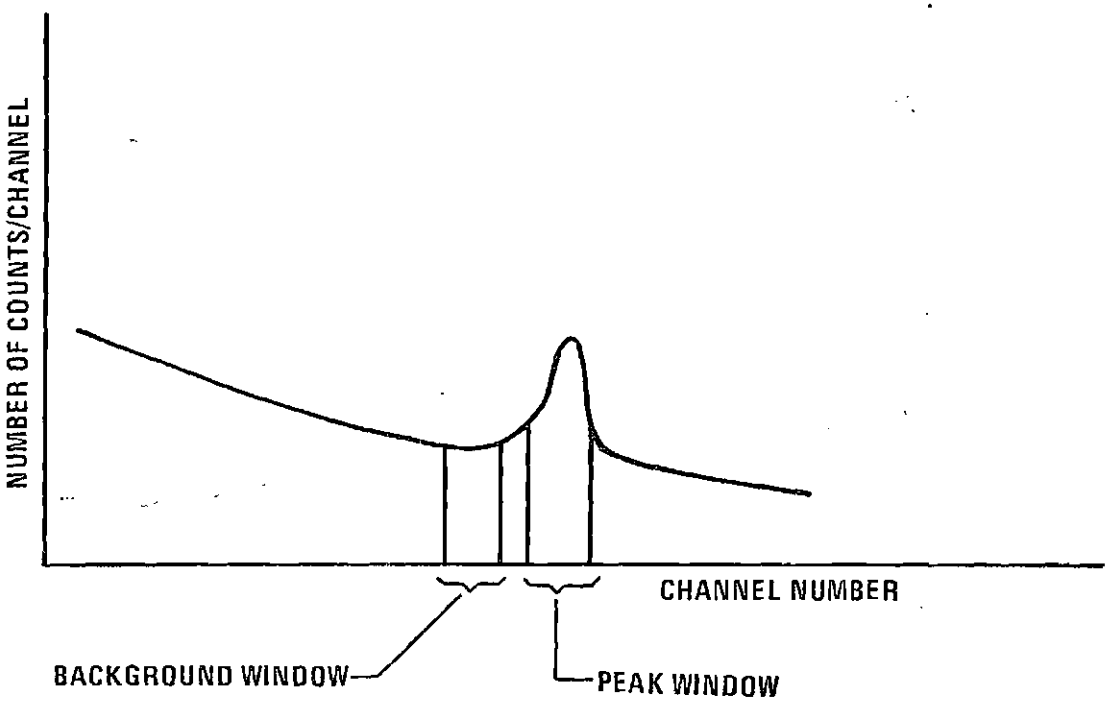


Figure 7. Compton Background Window Setting.

The spectra accumulated by MULTI were written on magnetic tape for later inspection. Another program (SEARCH) calculated the cross-correlation coefficient between the coincidence spectrum and a single gaussian peak of fixed width which was moved along the spectrum. A local maximum in the cross-correlation coefficient signified a match between the coincidence spectrum and the gaussian peak, and hence the location of a peak in the coincidence spectrum. The width of the gaussian was set equal to the expected linewidth for the energy region being searched; this linewidth increased with gamma energy, because of resolution degradation in the detector. SEARCH could not reliably locate weak or badly shaped peaks, however, so that some visual inspection of the coincidence spectra was necessary.

# CHAPTER V

## RESULTS FROM RADIATIVE CAPTURE IN $^{77}Se$

One gram of selenium powder enriched to 87.24 per cent in $^{77}Se$ (Oak Ridge Stable Isotopes, Oak Ridge, Tennessee) was placed in a cylindrical holder, 1/4 inch in diameter by 3/4 inch long, turned from aluminum. The target holder was closed by crimping the open end of the cylinder with an aluminum plug in place so that there was no need for adhesives, which might have contained elements with high capture cross sections. The target holder had a wall thickness of approximately 1/16 inch. This target was suspended in the thermal neutron beam as described in Chapter III.

### Energies of Gamma Rays

Singles spectra were taken in two runs, one a low-energy run covering the energy range 0.1 - 2.4 MeV and the other a high-energy run covering 5 - 11 MeV. Energy calibration was performed as described in Chapter IV; gamma ray energy standards used were obtained from pair-annihilation quanta and from thermal capture in nitrogen-14 contained in a melamine sample.

With the Georgia Tech Research Reactor operating at a thermal power level of one megawatt data on the low-energy portion of the spectrum were accumulated for a period of 75 minutes with the 30cc detector. The spectrum obtained is shown in Figure 8. As energy calibration standards the 511 keV annihilation peak and the double

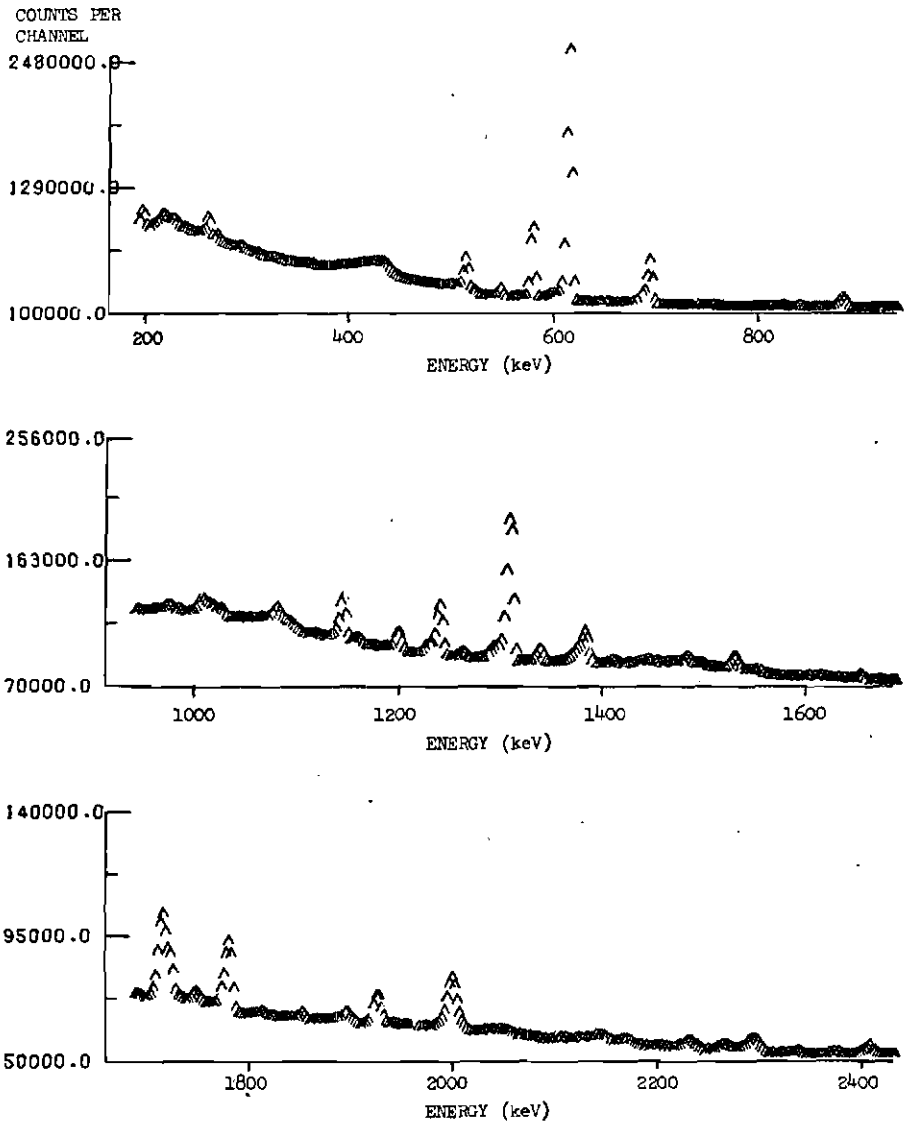


Figure 8. Low Energy Singles Gamma Ray Spectrum from Thermal Neutron Capture in $^{77}$Se.

escape peak at 2653 keV of the 3675 keV nitrogen capture line were used ( 54). After correction of the singles spectrum for drift the program GAUSS was used to fit the peaks with gaussian curves and the centroids, probable errors, and areas of the peaks were given to RAMPCL for correction of system nonlinearity and accurate energy calculation. The energies of the transitions attributed to decay of excited states in $^{78}$Se are given in Table 1. The paper of Rabenstein and Vonach (27 ) was invaluable for the identification of transitions due to other selenium isotopes.

High-energy spectra with both the selenium target and the melanine nitrogen target were taken in runs lasting 90 and 62 minutes, respectively. The high energy transitions attributed to $^{78}$Se decay are listed in Table 2, along with the calculated difference in the gamma ray energy and the neutron binding energy. This difference is the energy of the low-lying state populated by the transition whenever the transition is directly from the capture state. As shown in Chapter II, transitions with energies greater than 75 per cent of the binding energy may be assumed to be primary transitions, i.e., transitions directly from the capture state.

Gamma ray intensities were obtained by correcting, within RAMPCL, for detector efficiency variations. Full-energy-peak efficiencies were obtained using a set of standard radioisotopes (IAEA, Vienna).

The neutron binding energy was equal to the energy of a radiative transition from the capture state to the ground state, after correction for nuclear recoil. There was strong evidence to support the assignment of the 10494.4 keV transition as the ground state

Table 1. Energies and Intensities of Low-Energy Gamma Rays from Radiative Capture in $^{77}Se$

| Gamma Ray Energy (keV) | Intensity (Relative to 614 keV) |
|---|---|
| 194.5 | 1.76 |
| 499.9 | 1.40 |
| 545.8 | 2.55 |
| 578.8 | 24.24 |
| 614.4 | 100.0 |
| 690.9 | 11.98 |
| 695.9 | 16.03 |
| 768.0 | 0.74 |
| 828.9 | 1.50 |
| 845.7 | 1.31 |
| 887.1 | 10.84 |
| 1007.0 | 0.79 |
| 1081.0 | 1.22 |
| 1145.7 | 3.34 |
| 1199.8 | 2.06 |
| 1229.4 | 1.29 |
| 1296.0 | 2.06 |
| 1308.5 | 17.80 |
| 1372.6 | 1.85 |
| 1382.6 | 4.51 |
| 1530.3 | 2.14 |

Table 1. Energies and Intensities of Low-Energy Gamma Rays from Radiative Capture in $^{77}Se$ (Concluded)

| Gamma Ray Energy (keV) | Intensity (Relative to 614 keV) |
|---|---|
| 1653.5 | 0.77 |
| 1710.9 | 10.5 |
| 1921.2 | 3.21 |
| 1992.7 | 9.0 |
| 2182.8 | 0.64 |
| 2288.0 | 9.4 |
| 2394.6 | 1.85 |
| 2675.5 | 0.77 |

Table 2. Energies of High-Energy Gamma Rays from 78-Se and Low-Lying Levels Populated by Primary Transitions. (Intensities are not corrected for detector efficiency.)

| Gamma Ray Energy | Intensity | Level Energy |
|---|---|---|
| 10494.4 | 9.3 | 0 |
| 9880.3 | 100.0 | 614.1 |
| 9186.0 | 27.6 | 1308.4 |
| 8499.2 | 24.3 | 1995.2 |
| 8164.0 | 52.4 | 2330.4 |
| 7960.0 | 7.5 | 2534.4 |
| 7722.4* | 17.7 | 2772.0* |
| 7488.7 | 12.0 | (3005.7) |
| 7207.7 | 18.2 | (3286.7) |
| 7112.5 | 14.8 | (3381.9) |
| 6904.9 | 7.1 | (3589.5) |
| 6813.7 | 18.5 | (3680.7) |
| 6601.5 | 7.7 | (3892.9) |
| 6497.1 | 12.1 | (3997.3) |

*This transition includes a strong contribution from thermal capture in the aluminum target holder.

Note: Energy levels marked with ( ... ) are not assigned on the basis of primary transitions alone.

transition. It was the highest-energy gamma ray observed in the singles spectra. The 10494.4 keV transition also was not present in the total coincidence spectra, which were the spectra of all events in one detector which were in coincidence with any event in the other detector. The value of 10495.2 ± 3 keV is obtained as the neutron binding energy after recoil correction. This value agrees fairly well with the value of 10497.4 ± 1.2 keV of Rabenstein and Vonach (27) and with the value of 10491 ± 5 keV of Mattauch (55). The relatively large quoted error in the present value is attributed to drift in the gain and zero level of the spectrometry system between the selenium and melamine runs.

Assignment of gamma ray energies in Tables 1 and 2 was made on the basis of an inspection of the spectra for the full energy, single escape, and double escape peaks from each transition (56). Because of poor detector resolution at high energies and drift in the spectrometer the energy values in Table 2 have an associated error of several keV. Some disagreement between level energies based on primary transition energies and energy sums of gamma rays determined in the (more accurate ) low-energy runs was therefore expected.

## Coincidence Relationships

Two-parameter coincidence data were taken with the magnetic tape system described in Chapter III. The 30cc detector was set to accumulate the energy range 100 keV - 11 MeV; the 10cc detector covered the range 0 - 5 MeV. Runs lasting a total of 70 hours yielded nine 2400-foot reels of data on magnetic tape, which were sorted by the

computer program MULTI as discussed in Chapter IV. Coincidence gates were set on the 10cc spectrum for low-energy peaks and on the 30cc spectrum for high-energy peaks. Figure 9 shows representative coincidence spectra and illustrates that unambiguous coincidence relationships could be easily established for all except quite weak cascades. The spectra shown have been corrected for Compton background coincidences but not for contributions from chance coincidences (37). However, inspection of the time spectra for these runs showed that the ratio of true to chance coincidences was at least 10:1.

Coincidence relationships established in these runs are listed in Table 3. Those relationships denoted by ( ? ) were established from weak coincidence peaks and are not claimed to be unambiguous.

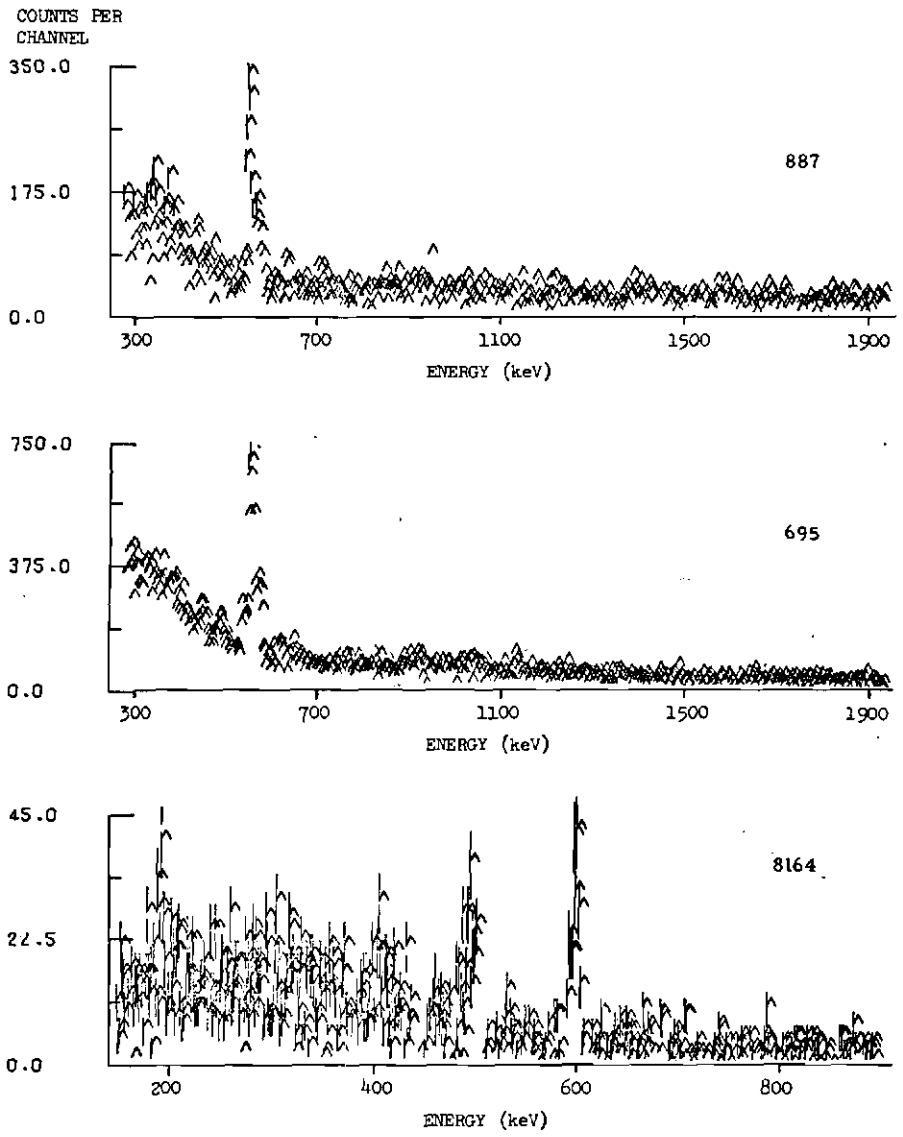


Figure 9. Representative Low Energy Coincidence Gamma Ray Spectra from Thermal Neutron Capture in $^{77}$Se. (The label on each spectrum gives the energy of the transition with which the spectrum was in coincidence).

Table 3. Coincidence Relationships Among Radiative Transitions in $^{78}Se$

| Gamma Ray Energy (keV) | Coincidence Gamma Ray Energy (keV) |
|---|---|
| 614 | 695, 885, 1145, 1241(?), 1681, 9880, 9184(?), 8164, 7208 |
| 695 | 545, 828, 614, 1199, 9184 |
| 1309 | 9184 |
| 1713 | 8164, 614 |
| 885 | 614, 768(?), 8164(?) |
| 7208 | 614, 2674, 694 |
| 7489 | 614, 694, 1304(?), 2386(?) |
| 8164 | 614, 1713(?), 209(?) |

Note: Transitions marked with (?) are present only weakly in the coincidence spectra and their placement in the decay scheme is based partly on energy and intensity balances.

# CHAPTER VI

## THE DECAY SCHEME OF $^{78}$Se

From the singles and coincidence data given in the preceding chapter the level scheme shown in Figure 10 was deduced. Only a partial decay scheme is shown, meaning that some levels populated in other reactions but not seen in the present work are not included. This actually was not an important restriction on the level scheme of $^{78}$Se since essentially all the very low-lying levels known in this isotope were populated by thermal neutron capture.

The level scheme was constructed by first assuming the existence of levels with energies determined from the difference between the neutron binding energy and the energies of primary transitions (Table 2). Then the levels at 1500 keV, 1758 keV, 1854 keV, and 2682 keV, whose existence was well supported by previous studies (18,19,27), as well as by gamma ray energy sums from the present work were added. Finally low-energy transitions from Table 1 were fitted into this level scheme in order to construct a decay scheme. A transition had to meet two requirements in order to qualify for placement between two levels in the nuclear level scheme. It must first have had an energy equal to the difference in the level energies, within the limits of probable experimental error. If a new level was being proposed, the imposition of this requirement on all tentatively assigned transitions to or from the level led to the consideration of cross-over energy sums.

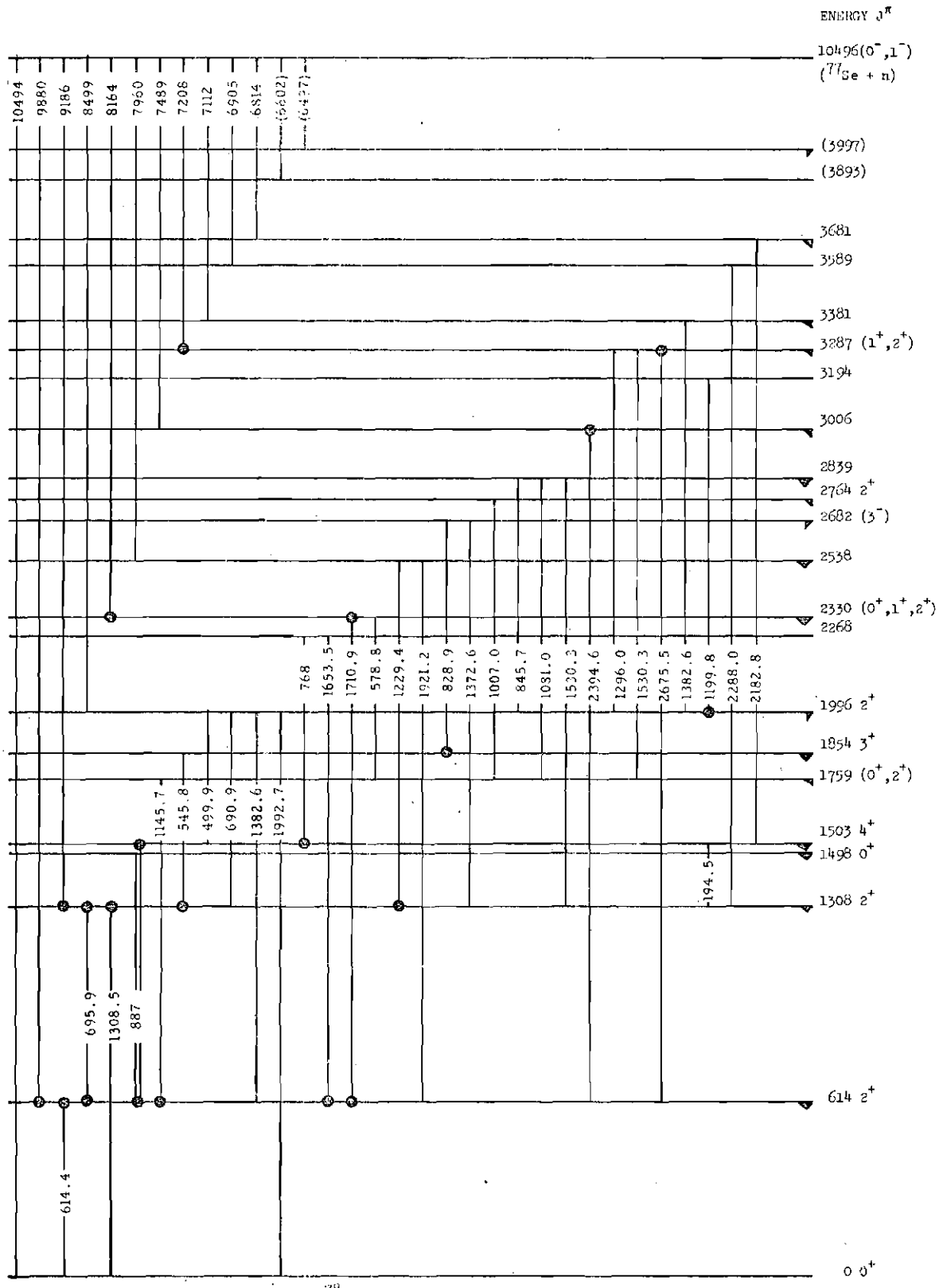


Figure 10. Proposed Decay Scheme of $^{78}$Se Deduced from Coincidence and Singles Gamma Ray Data of the Present Work. (The excitation energies are expressed in keV. Those levels marked on the right with ◥ have been observed in previous radioactive decay studies; those marked with ◤ have been observed in (p,p), (d,p) or alpha particle stripping reactions. The spins and parities to the right of the excitation energies are taken from References 19 and 27. Both at the beginning or end of an arrow representing a transition indicate an observed coincidence between the transition so marked and other gamma rays proceeding to or from the same level, respectively.)

As an example, the level at 2682 keV, not directly populated from the capture state, is assumed to decay by at least two branches to the level at 1308 keV: a transition of 828.9 keV to the 1854 keV level followed by one of 545.8 keV to the 1308 keV level, and a direct transition of 1372.6 keV. This assumption was checked and substantiated by noting that the sum of the two transitions in the cascade was 1374.7 keV, which was within 2 keV, a possible experimental error, of the energy of the direct transition. That not all energy sums in the proposed scheme agreed to better precision than this example was due to experimental errors in the energy values, as discussed in Chapter V. The second requirement for placement of a transition in a level scheme was that its intensity, together with the intensities of other proposed transitions to and from the level, had to satisfy a simple balance condition: The sum of the intensities entering a level was required to be less than or equal to the sum of the intensities of transitions depopulating the level. That this was usually only approximately satisfied was due not only to errors in the determination of gamma ray intensities but also to the fact that often a level, especially a high-lying one, was fed or depopulated by many very weak transitions which were unobserved. In practice the intensity balance requirement was less well satisfied than the energy balance requirement, even for very low-lying levels, because an accurate determination of the intensity of a gamma ray was more difficult than the determination of its energy. The present neutron capture data had an error of about 0.5 keV in energy determinations, on the order of a small fraction of a percent, but intensities were known to only 5 to

10 per cent accuracy. A glaring example of intensity imbalance in the present decay scheme was the level at 3997 keV, to which no transition could be unambiguously assigned for depopulation, although the 6497 keV transition to this level was seen. The level was included because of the observed 6497 keV primary transition. Other workers (27) had assigned as many as four transitions between this and lower-lying levels (none of them, however, on the basis of coincidence data).

As recently as 1970 the levels at 1498 keV and 1503 keV were assumed to be a single level, with spin assignments differing with different modes of population (57). Rabenstein and Vonach (27) showed clearly that the level was a doublet with a 4+ state at 1503 keV and 0+ state at 1498 keV. This result also removed one problem in the level systematics of the selenium isotopes, that $^{78}$Se should have been a vibrational nucleus but that only two of the three members of the two-phonon triplet were observed (57).

The transition at 194.5 keV, expected on the basis of theoretical considerations as explained below, has not been previously reported. Its assignement is supported on two grounds: First, energy balance is well satisfied. Using energy values from the present work agreement to within 2 keV is obtained and with the level energies of Rabenstein and Vonach agreement to within 0.3 keV results. Second, the possibility that this transition might be in the nucleus $^{77}$Se, excited by thermal capture in the large amount of $^{76}$Se in the target, is ruled out on the following grounds. One transition which can be definitely

assigned to $^{77}$Se is observed, at 238.2 keV. The only strong transition in $^{77}$Se near 194 keV is at 200.4 keV (27). The ratio of the intensities of the 238 keV and 200 keV transitions in $^{77}$Se is 27:3. The ratio of the 238 keV and 194 keV transitions in the present work was, however, 1.85:1.76, so that the 194 keV line may be assigned with confidence to $^{78}$Se.

Coincidence data are of great value in checking tentative assignments of transitions within a level scheme. As an example, suppose that two transitions had been tentatively assigned as depopulating the same level. The observation of these two lines in coincidence would invalidate this assignment, but would yield the further information that these two transitions must have either a common intermediate level or one or more intermediate transitions which fed intensity from one of the transitions to the other.

Data from the coincidence runs in the present work (Table 3) have allowed the removal of an ambiguity in the best previous thermal capture level scheme (27) and have shown one tentative assignment in that work to be questionable.

The transition of 768 keV was placed twice in the decay scheme of Rabenstein and Vonach (27), since energy sums were satisfied in both positions and the transition was not observed in their coincidence data. The transition was observed in coincidence in the present work, albeit weakly, so that one of the two prior placements is more likely than the other. The observation of the 768 keV transition in coincidence with the 885 keV line makes its assignment at 2765 keV - 1996 keV

less likely than the lower placement at 2268 - 1500 keV. This follows if one considers the relationship between the upper placement and the 885 keV transition: The upper placement has this transition feeding the 1996 keV level, which decays with very low intensity to the 1500 keV level. The intermediate transition at 500 keV was not observed in coincidence with the 885 keV transition, so that there is no evident way for intensity to be fed from the upper placement of the 768 keV transition to the 885 keV transition, with which it is in coincidence.

In the work of Rabenstein and Vonach (27), the decay scheme of $^{78}$Se was a by-product of their principal work on the $^{77}$Se level scheme. Capture was in natural selenium, so that the preponderance of capture was $^{76}$Se(n,$\gamma$)$^{77}$Se. In addition, the fact that $^{77}$Se is an odd nucleus means that there was a plethora of low-energy gamma rays in their work which had to be apportioned between $^{77}$Se and $^{78}$Se. Many transitions were overlaid by other full-energy or double escape peaks. Their assignment of a transition of 1010.4 keV to the levels 3006 keV - 1996 keV was thus highly tentative. As seen in Table 3, no transition of 1010 keV was observed in the present work in coincidence with the 7489 keV gamma ray which fed the 3006 keV level, nor was a transition of this energy observed with appreciable intensity in either the total coincidence spectra or the singles energy determination spectrum. A transition of 2034 keV was seen in $^{77}$Se by Rabenstein and Vonach, and its double escape peak would coincide closely with a transition at 1010.4 keV. Thus, while the assignment of a 1010.4 keV transition to the $^{78}$Se level scheme is not ruled out by the present work, it is rendered highly questionable.

## Discussion

Theoretical papers on the selenium isotopes are not as abundant as those on some other nuclei. One of the principal reasons is that these isotopes are not clear-cut examples of either collective or single-particle behavior, although the level scheme can be generally characterized as a vibrational one. The pioneering application of the BCS theory ( 58) to systematics over wide mass regions by Kisslinger and Sorensen ( 59) cites the selenium isotopes along with many others. They showed that for a linearized quasi-random-phase approximation to the vibrational collective structure the hindrance of the transition rate from the second 2+ excited state to the ground state in comparison with the rate of the first-2+ to ground state transition could be qualitatively reproduced, although the corrections to the simple quasiparticle theory were of such magnitude as to make quantitative prediction difficult. Briefly, a phenomenological explanation of the hindrance of this so-called crossover transition is that the ground state has no vibrational excitation, and is a zero-phonon state; the first excited 2+ state is a one-phonon vibrational excitation, and the second 2+ state is a two-phonon excitation (as are the second 0+ state and the first 4+ state, in general). A transition from the second 2+ state to the ground state then involves two phonons which makes it a less likely transition than a one-phonon transition from the first 2+ state to the ground state. This effect totally overrides the single-particle transition probability prediction; i.e., that transition probabilities will be proportional to the fifth power of the energy for E2 radiation ( 33). In the case of $^{78}$Se, the energies of the

transitions are 1308 keV and 614 keV; the single-particle model predicts that their transition probabilities will be in the ratio 44:1. Their observed intensities, however, are in the ratio 0.18:1. It is thus clear that these levels have very little single-particle character and are collective in nature.

The nature of this collective motion is well described by saying that the low-lying collective levels are analogous to those of an anharmonic oscillator, as explained in Chapter I. The transition of 194.5 keV found in this work, from the first 4+ level to the second 2+ level, is within the 0+, 2+, 4+ two-phonon triplet. A harmonic oscillator has these three levels degenerate so that no transitions among them could occur; the observation of such a transition, then, is an indication of anharmonicity. The fact that the second 2+ level is split almost 200 keV away from the other two triplet members in $^{78}$Se means that there should be some branching from the higher-energy members to the lower-energy members of the two-phonon triplet. An even more complex situation is found (60) in the level structure of $^{116}$Sn, where the triplet splitting is larger (on the order of 360 keV) and more nearly equal, and transitions are observed among all three triplet members. Theoretically it would be of interest to obtain separate transition intensities for the 4+ - 2+ and the 0+ - 2+ transitions, but the upper two states in $^{78}$Se are so nearly degenerate that the two transitions could not be resolved in the present work. An extremely high resolution study of the 194.5 keV line might yield the desired branching ratios, however. Some theorists feel that the two-phonon vibrational model is too phenomenological (61), but whatever theory is used branching ratios among these low-lying collective states will be of interest.

A recent study by Leider and Draper (24) is also of interest. They used alpha particle stripping reactions, which populated preferentially quasirotational states. Very good agreement between their energy values and predictions of a rotational model was obtained, so that the selenium isotopes behave rotationally for high collective excitation energies. The quasirotational band includes the same low-lying states which we have already seen are well described by a vibrational model. The nucleus may be thought of as stretching into a distorted shape at high excitations, but it is probably preferable to ignore the simple phenomenological vibrational description for all except the very lowest levels. Future experimental work might explore the rotational-vibrational coupling in the region from two to four MeV, a region in which experimental data are becoming more readily obtainable due to improved instrumentation.

# CHAPTER VII

## CONCLUSIONS AND RECOMMENDATIONS

Two principal conclusions may be drawn from the thermal neutron capture work reported in this thesis. First, it has been demonstrated that the thermal capture facility constructed at the Georgia Institute of Technology is capable of performing radiative capture decay scheme studies comparable in quality to those reported by established laboratories, although several improvements would be desirable. It is especially noteworthy that the multiparameter data acquisition system was constructed with a moderate amount of effort and at quite reasonable cost (approximately $7,000) using standard commercial components exclusively. Multiparameter experiments, which are becoming more and more necessary with high-resolution detectors, are thus within the reach of a number of laboratories. Previous multiparameter systems (46) were expensive, unreliable, and slow by comparison. Further, the use of magnetic tape data storage and off-line data reduction allowed 4096 by 4096 channel coincidence resolution, whereas systems using online computer disk storage for multiparameter experiments (62) are not only more expensive but are restricted to 512 by 512 or fewer channels.

The second conclusion which can be drawn from this work is that the principal recent decay scheme studies on the nucleus $^{78}$Se are in the main correct, with the exceptions noted in the discussion of

Chapter VI, but that further work is needed both to clear up existing ambiguities and to extend the scheme to higher-lying levels. The present work, the papers of Rabenstein and Vonach (27), of Morcos, Ward, and Kuroda (19), and of Paradellis and Hontzeas (18), as well as earlier work summarized by Artna (26), are in good agreement on the lowest-lying energy levels and on the vibrational character of the excitations of these lowest levels. That an ambiguity in the decay scheme of Rabenstein and Vonach was removed by the present study in some consolation for the fact that at least one new ambiguity, the placement of the 1010.4 keV transition, has been pointed out.

Generalizations based on initial acquaintance with a field of research are of dubious value in actually guiding the direction of subsequent work. However, a different viewpoint does allow questions to be raised whose consideration might be beneficial.

One conclusion drawn from the progress of this work is that radiative capture decay scheme studies, in attempting to elucidate increasingly more subtle details of the structures of a wider range of nuclei, will require constant effort toward improving the performance of the spectrometry system; (n,$\gamma$) studies are one important area in which the "state of the art" in detectors, data acquisition systems, and neutron sources is constantly being challenged. Data from this work which support this conclusion include the observation that even a relatively moderate improvement in detector resolution would have allowed the unambiguous placement of more transitions in the decay scheme. It was also evident during the course of these experiments that noise, drift, and nonlinearities in the signal processing system reduced the

effective resolution of the detectors to a noticeable extent. This state of affairs is not always present in other areas of nuclear spectroscopy which yield data complementary to that found in the present type of work, where instrumentation of moderate performance may be quite adequate to obtain desired results.

It is recommended that decay scheme studies be augmented by other types of research in which a large, continuing investment of equipment, effort, and time is not required. An automated angular correlation apparatus could be constructed, making use of a small on-line computer in place of the present multichannel analyzer, which would ideally operate unattended for long periods of time. Data on the more detailed properties of nuclear states and transitions, such as multipole mixing ratios, could be obtained for fairly weak cascades if Ge(Li) detectors were used exclusively and long data acquisition runs employed.

Electron spectroscopy would be a fascinating adjunct of gamma-gamma coincidence studies, either in internal conversion coincidence and correlation studies or in the newly emerging field of internal pair production spectroscopy (63). It appears, however, that a large investment in equipment and time would be required.

It seems advisable that more effort be expended on practical applications of research techniques and results. Radiative capture is being explored as an alternative to conventional neutron activation analysis (64) and the existing thermal capture facility and instrumentation are well suited to developmental research on this new analytical technique.

Other possibilities for challenging work are perturbed angular correlations (65) using thermal capture excitation of a particular element in a compound as an extension of existing magnetic resonance spectroscopy in chemistry and biology (see the discussion by Klein (66), and Mossbauer studies with capture gammas (67).

BIBLIOGRAPHY


1. Baranger, M., Bull. Am. Phys. Soc., 16, 486 (1971).

2. Brown, G. E., Unified Theory of Nuclear Models, 2nd edition, North-Holland, Amsterdam, 1967.

3. Siegbahn, K., ed., Alpha- , Beta- , and Gamma-Ray Spectroscopy, North-Holland, Amsterdam, 1966.

4. McClure, D. A., and J. W. Lewis, Bull. Am. Phys. Soc., 16, 495 (1971).

5. Motz, H. T., Neutron Capture Gamma Ray Spectroscopy, in E. Segre, ed., Ann. Rev. Nucl. Sci. 1970, Annual Reviews, Palo Alto, 1970.

6. Bergqvist, I., and N. Starfelt, Neutron Capture Gamma Rays, in D. M. Brink, ed., Progress in Nuclear Physics, 11, Pergamon, Oxford, 1970.

7. Neutron Capture Gamma-Ray Spectroscopy, International Atomic Energy Agency, Vienna, 1969.

8. Bollinger, L. M., Some Aspects of Neutron Capture Gamma Rays, Argonne National Laboratory Informal Report PHY-1970C, Argonne, 1970.

9. Gibson, W. M., G. L. Miller, and P. F. Donovan, in K. Siegbahn, ed., Alpha-, Beta- , and Gamma-Ray Spectroscopy, North-Holland, Amsterdam, 1966.

10. Bolotin, H. H., in Neutron Capture Gamma-Ray Spectroscopy, International Atomic Energy Agency, Vienna, 1969.

11. Bohr, A., B. Mottelson, and D. Pines, Physical Review, 110, 936 (1958).

12. Belyaev, S. T., Mat. Fys. Medd. Dan. Vid. Selsk. 32, no. 11 (1959).

13. Nathan, O., and S. G. Nilsson, in K. Siegbahn, ed., Alpha-, Beta-, and Gamma-Ray Spectroscopy, North-Holland, Amsterdam, 1966.

14. Bohr, A. and B. R. Mottelson, Nuclear Structure, vol. 3, Benjamin, New York, to be published.

15. Kelson, I., and C. A. Levinson, Physical Review, 134, B269 (1964).

16. Brink, D. M., and E. Boeker, Nuclear Physics, A91, 1,(1967).

17. Faessler, A., P. U. Sauer, and H. H. Wolter, Nuclear Physics, A129, 21 (1969).

18. Paradellis, T., and S. Hontzeas, Nuclear Physics, A142, 204 (1970).

19. Morcos, N. A., T. E. Ward, and P. K. Kuroda, Nuclear Physics, A168, 561 (1971).

20. Adler, K., A. Bohr, T. Huus, B. Mottelson, and A. Winther, Reviews of Modern Physics, 25, 729 (1953).

21. Bygrave, W., D. Eccleshall, and M. I. L. Yates, Nuclear Physics, 53, 385 (1964).

22. Lin, E. K., Physical Review, 139, B340 (1965).

23. Darcey, W., D. I. Pullen, N. W. Tanner, in E. Clemental, ed, Direct Interactions and Nuclear Reaction Mechanisms, Gordon and Breach, New York, 1963.

24. Lieder, R. M., and J. E. Draper, Physical Review C, 2, 531 (1970).

25. Bartholomew, G. A., A. Doveika, K. M. Eastwood, and S. Monaro, Nuclear Data, 3, 367 (1967).

26. Artna, A., Nuclear Data B, 1, B1-4 (1966).

27. Rabenstein, D., and H. Vonach, Zeitschrift fur Naturforschung, to be published.

28. Rowe, D. J., Collective Nuclear Motion, Methuen, London, 1970, pp. 16-25.

29. Chadwick, J., Proceedings of the Royal Society, A, 142, 1 (1933).

30. Hughes, D. J., and J. A. Harvey, Neutron Cross Sections, United States Atomic Energy Commission - McGraw-Hill, New York, 1955, pp. 186-187.

31. Bohr, N., Nature, 137, 344 (1936).

32. Bollinger, L. M., Physical Review C, 3, 2071 (1971).

33. Preston, M. A., Physics of the Nucleus, Addison-Wesley, New York, 1962.

34. Porter, C. E., and R. G. Thomas, Physical Review, 104, 483 (1956).

35. Wigner, E. P., Annals of Mathematics, 67, 325 (1958).

36. Porter, C. E., and N. Rosenzweig, Ann. Acad. Sci. Finland, A6, no. 44 (1960).

37. Mehta, M. L., Random Matrices, Academic Press, New York, 1967.

38. Bohr, A. and B. R. Mottelson, Nuclear Structure, vol. 1, Benjamin, New York, 1969, p. 300.

39. Messiah, A., Quantum Mechanics, John Wiley & Sons, New York, 1966, p. 290.

40. Feller, W., An Introduction to Probability Theory and Its Applications, John Wiley and Sons, New York, 1962, p. 200.

41. Bollinger, L. M., in Nuclear Structure, International Atomic Energy Agency, Vienna, 1968.

42. Preston, M. A., Physics of the Nucleus, Addison-Wesley, New York, 1962, p. 18.

43. Wapstra, A. H., The Coincidence Method, in K. Siegbahn, ed., Alpha-, Beta-, and Gamma-Ray Spectroscopy, North-Holland, Amsterdam, 1966.

44. Strauss, M. G., I. S. Sherman, R. Brenner, S. J. Rudnick, R. N. Larsen, and H. M. Mann, Review of Scientific Instruments, 38, 725 (1967).

45. Final Safeguards Report, Georgia Tech Research Reactor, Atlanta, 1963.

46. McClure, D. A., Argonne National Laboratory Informal Report PHY-1969E, Argonne, 1969.

47. Fairstein, E., and J. Hahn, Nucleonics, 23, 56 (1965), 24, no. 1, 54 (1966).

48. Strauss, M. G., F. R. Lenkszus, and J. J. Eichholz, Bull. Am. Phys. Soc., 14, 531 (1969).

49. Michaelis, W., and F. Horsch, in Neutron Capture Gamma Ray Spectroscopy, I. A. E. A., Vienna, 1969.

50. Davidon, W. C., Argonne National Laboratory Report ANL-5990 (Rev. 2), 1966.

51. Stewart, G. W., Journal of the Association for Computing Machinery, 14, 72 (1967).

52. Fletcher, R., and J. J. D. Powell, Computer Journal, 6, 163 (1963).

53. Fubini, A., M. Giannini, E. Ivanov, M. Popa, D. Prosperi, and V. Rado, in Neutron Capture Gamma Ray Spectroscopy, I. A. E. A., Vienna, 1969.

54. Van Asche, P. H. M., in Neutron Capture Gamma-Ray Spectroscopy, International Atomic Energy Agency, Vienna, 1969.

55. Mattauch, I. E. H., Nuclear Physics, 67, 32 (1965).

56. Gibson, W. M.,G. L. Miller, and P. F. Donovan, Semiconductor Particle Spectrometers, in Alpha-, Beta-, and Gamma-Ray Spectroscopy, ed, K. Siegbahn, North-Holland, Amsterdam, 1966.

57. Eisenberg, J. M. and Greiner, Nuclear Models, North-Holland, Amsterdam, 1971.

58. Bardeen, J., L. N. Cooper, and J. R. Schrieffer, Physical Review, 108, 1175 (1957).

59. Kisslinger, L. S., and R. A. Sorensen, Reviews of Modern Physics, 35, 853 (1963).

60. Rabenstein, D., Zeitschrift für Physik, 240, 244 (1970).

61. Rasmussen, J. O., in Nuclear Structure, International Atomic Energy Agency, Vienna, 1968; also Private Communication.

62. Harratz, D., J. Glatz, and K. E. G. Lobner, to be published.

63. Allan, C. J., Canadian Journal of Physics, 49, 157 (1971).

64. Walker, D., and D. A. McClure, Private Communication.

65. Karlsson, E., E. Matthias, and K. Siegbahn, eds., Perturbed Angular Correlations, North-Holland, Amsterdam, 1964.

66. Klein, M. P., in Report of the Chemical Biodynamics Group, Lawrence Radiation Laboratory, Berkeley, 1970.

67. Goldanskii, V. I., and R. H. Herber, eds., Chemical Applications of Mossbauer Spectroscopy, Academic Press, New York, 1968, p. 642.

# VITA

John Wiley Lewis III was born in Birmingham, Alabama on June 15, 1945. He attended Phillips High School in Birmingham and was graduated in 1962 as valedictorian and class president. In June 1966 he was awarded the Bachelor of Science in Physics, with honor, by the Georgia Institute of Technology. While at Georgia Tech he received the Pursley Award as the outstanding senior physics major and was a member of Omicron Delta Kappa, Phi Kappa Phi, Sigma Pi Sigma, Tau Beta Pi, and Pi Tau Chi honorary fraternities.

During the academic year 1966-67 he attended the Eidgenössische Technische Hochschule in Zurich, Switzerland as a World Student Fund Fellow. In September 1967 he was enrolled in the Graduate Division of the Georgia Institute of Technology, obtaining the degree Master of Science in Physics in 1968. During the academic year 1970-71 he was a National Science Foundation Predoctoral Trainee.

Mr. Lewis married Nancy Hartman Hotchkiss in 1968 and they have one child, Katherine Hunt Lewis.